

# Genesis of the Jiajika superlarge lithium deposit, Sichuan, China: constraints from He–Ar–H–O isotopes

Tao Liu<sup>1,2,3</sup> · Hai Wang<sup>1</sup> · Shihong Tian<sup>1,4</sup> · Denghong Wang<sup>4</sup> · Xianfang Li<sup>4</sup> · Xiaofang Fu<sup>5</sup> · Xuefeng Hao<sup>5</sup> · Yujie Zhang<sup>4,6</sup> · Kejun Hou<sup>4</sup>

Received: 29 September 2022 / Revised: 24 December 2022 / Accepted: 28 December 2022 / Published online: 12 January 2023  
© The Author(s), under exclusive licence to Science Press and Institute of Geochemistry, CAS and Springer-Verlag GmbH Germany, part of Springer Nature 2023

**Abstract** The Jiajika granitic- and pegmatite-type lithium deposit, which is in the Songpan–Garze Orogenic Belt in western Sichuan Province, China, is the largest in Asia. Previous studies have examined the geochemistry and mineralogy of pegmatites and their parental source rocks to determine the genesis of the deposit. However, the evolution of magmatic-hydrothermal fluids has received limited attention. We analyzed He–Ar–H–O isotopes to decipher the ore-fluid nature and identify the contribution of fluids to mineralization in the late stage of crystallization differentiation. In the Jiajika ore field, two-mica granites, pegmatites (including common pegmatites and spodumene pegmatites), metasandstones, and schists are the dominant rock types exposed. Common pegmatites derived from early differentiation of the two-mica granitic magmas before they evolved into spodumene pegmatites during the

late stage of the magmatic evolution. Common pegmatites have  $^3\text{He}/^4\text{He}$  ratios that vary from 0.18 to 4.68 Ra (mean 1.62 Ra), and their  $^{40}\text{Ar}/^{36}\text{Ar}$  ratios range from 426.70 to 1408.06 (mean 761.81); spodumene pegmatites have  $^3\text{He}/^4\text{He}$  ratios that vary from 0.18 to 2.66 Ra (mean 0.87 Ra) and their  $^{40}\text{Ar}/^{36}\text{Ar}$  ratios range from 402.13 to 1907.34 (mean 801.65). These data indicate that the hydrothermal fluids were shown a mixture of crust- and mantle-derived materials, and the proportion of crust-derived materials in spodumene pegmatites increases significantly in the late stage of the magmatic evolution. The  $\delta^{18}\text{O}_{\text{H}_2\text{O}-\text{VSMOW}}$  values of common pegmatites range from 6.2‰ to 10.9‰, with a mean value of 8.6‰, and  $\delta\text{D}_{\text{V}-\text{SMOW}}$  values vary from –110‰ to –72‰, with a mean of –85‰. The  $\delta^{18}\text{O}_{\text{H}_2\text{O}-\text{VSMOW}}$  values of spodumene pegmatites range from 5.3‰ to 13.2‰, with a mean of 9.1‰, and  $\delta\text{D}_{\text{V}-\text{SMOW}}$  values vary from –115‰ to –77‰, with a mean of –91‰. These data suggest that the ore-forming fluids came from primary magmatic water gradually mixing with more meteoric water in the late stage of the magmatic evolution. Based on the He–Ar–H–O and other existing data, we propose that the ore-forming metals are mainly derived from the upper continental crust with a minor contribution from the mantle, and the fluid exsolution and addition of meteoric water during the formation of pegmatite contributed to the formation of the Jiajika superlarge lithium deposit.

✉ Shihong Tian  
tshhong@ecut.edu.cn

<sup>1</sup> State Key Laboratory of Nuclear Resources and Environment, East China University of Technology, Nanchang 330013, China

<sup>2</sup> Changsha Uranium Geology Research Institute, CNNC, Changsha 410007, China

<sup>3</sup> Hunan Engineering Technology Research Center for Evaluation and Comprehensive Utilization of Associated Radioactive Mineral Resources, Changsha 410007, China

<sup>4</sup> MNR Key Laboratory of Metallogeny and Mineral Assessment, Institute of Mineral Resources, Chinese Academy of Geological Sciences, Beijing 100037, China

<sup>5</sup> Geological Survey of Sichuan Province, Chengdu 610081, China

<sup>6</sup> School of Earth Science and Mineral Resources, China University of Geosciences, Beijing 10083, China

**Keywords** He–Ar–H–O isotopes · Magmatic–hydrothermal fluids · Common pegmatites · Spodumene pegmatites · Jiajika superlarge lithium deposit, Sichuan

## 1 Introduction

Lithium (Li) is the lightest metal element with high melting and boiling point, which is widely used in batteries, ceramics, glass, lubricating greases, electronics, metallurgy, and medical and optical industries (USGS 2021). China, the United States, and Europe have treated Li as one of the important critical metal resources, which are of growing economic importance (Goodenough 2017; Zhai et al. 2019; European Commission 2020). Pegmatites are one of the important sources of rare metals, including lithium, beryllium, tantalum, niobium, rubidium, cesium, zirconium, hafnium, wolfram, and tin (London 2014; Dill 2015; Fei et al. 2017; Liu et al. 2020b). Thus, they are important targets in rare-metal exploration (Wang et al. 2004, 2005). Although granitic-pegmatites are common, rare-metal pegmatites make up only ~ 0.1% of the total amount of these rocks, and Li-rich pegmatites are still rarer (Laznicka 2006; Kesler et al. 2012; Linnen et al. 2012). Pegmatites are commonly thought to form from residual magmas through the differentiation of granitic magmas (Černý and Ercit 2005; London 2008; Deveaud et al. 2015; Roda-Robles et al. 2018; Wang et al. 2020; Yan et al. 2020; Hu and Li 2021). However, other pegmatites are the result of anatexis. (Deveaud et al. 2015; Barros and Menug 2016; Dill 2018; Knoll et al. 2018; Hu and Li 2021). Consequently, a close temporal or spatial relationship between granites and pegmatites does not necessarily indicate a comagmatic origin (Muller et al. 2017).

Many pegmatite-type lithium deposits have been found in China and most of them are distributed in Songpan-Ganze, Chinese Altay, and Jiangnan orogenic belts (Li et al. 2014; Wang et al. 2017a, b). The Songpan–Ganze Orogenic Belt (SGOB), located in the western part of Sichuan province, China, is one of the most important lithium deposits producing areas (Fig. 1). The main pegmatite-type deposits in the SGOB include the Dangba rare-metal and muscovite deposits, Lijiagou rare-metal deposit, Ke’eryin rare-metal deposits and Jiajika lithium deposit (Wang et al. 2005, 2013; Li 2006; Li et al. 2014, 2015a, b; Fei et al. 2017, 2020a, 2021), and the Jiajika deposit is the largest known granite- and pegmatite-type Li deposit within Asia. The deposit was discovered by the Ganzi Geological Prospecting Team of the Sichuan Bureau of Geology and Mineral Resources Exploration in 1959. Subsequent detailed exploration showed that the total Li<sub>2</sub>O resource reached 2.81 million tons (Li and Chou 2017). Numerous studies have investigated the timing of petrogenesis and mineralization, magmatic origin, metallogenic regularities, and continental geodynamics of this deposit (Li et al. 2006a, b, c, d, 2007a, 2008a, b, 2014, 2020; Su et al. 2011; Fu et al. 2014, 2015; Hao et al. 2015; Liu et al.

2015, 2016, 2017a, b, c; Liang et al. 2016; Hou et al. 2017; Wang et al. 2017a, b; Dai et al. 2018a, b; Huang et al. 2020). However, issues related to fluid evolution, metal source, and metallogenic mechanisms remain poorly constrained. Previous studies on hydrothermal fluids of pegmatites are limited to some specific ore bodies (Xiong et al. 2019; Zhou et al. 2021; Wang et al. 2022), and the properties and sources of hydrothermal fluids of common pegmatites are not clear. Zhang et al. (2021) revealed that fluid exsolution during melt-fluid separation can cause significant Li isotopic fractionation between common and spodumene pegmatites using lithium isotopes. Therefore, more studies are needed on the fluid inclusion of the pegmatite-type lithium deposits, these studies are crucial for the origin and enrichment mechanisms of Li in the Jiajika district.

He–Ar isotopes of inclusion-trapped fluid have been studied for several decades, and are powerful tools for tracing fluid sources and mixing processes between mantle volatiles and crustal fluids during the formation of metal deposits (Schlutter et al. 1987; Turner et al. 1992, 1993a, b; Stuart et al. 1995; Hu et al. 1997, 1998, 1999, 2004, 2009, 2012; Burnard et al. 1999; Li et al. 2007b, 2010, 2011, 2018; Sun et al. 2009; Wu et al. 2011; Chen et al. 2018). <sup>40</sup>Ar/<sup>36</sup>Ar ratios differ between atmospheric and crust/mantle. The <sup>3</sup>He/<sup>4</sup>He ratios of mantle-derived fluids (6–7 Ra) can be 1000 times higher than those of crust-derived fluids (0.01–0.05 Ra) (Stuart et al. 1995). This large difference in He isotope ratios makes it even easier to identify minor mantle-derived He in fluids (Hu et al. 1998, 2009, 2012; Sun et al. 2009). Thus, He–Ar isotopes can be used to effectively indicate the sources of hydrothermal fluids in ore deposits (Xu et al. 2014; Zhai et al. 2015). In addition, H–O isotope data also can provide clues to the nature of magmatic-hydrothermal fluids (Chen et al. 2009; Hou et al. 2009; Wang et al. 2018a, b).

Herein, we report the geological characteristics of the Jiajika superlarge lithium deposit and use He–Ar–H–O isotope data to determine the source of the mineralizing fluids. Along with our previous results, we reconstruct the successive processes that led to the mineralization of the Jiajika superlarge lithium deposit from the magmatism to fluid evolution and focused on the fluid exsolution and meteoric water in this study.

## 2 Geological setting, deposit geology, and samples

The Jiajika superlarge spodumene deposit is located at the eastern margin of the Qinghai–Tibet Plateau and in the central SGOB (Fig. 1). The SGOB formed as a result of tectonic interactions between South China, North China, and Qiangtang blocks during the closure of the Paleo-Tethys Ocean (Fig. 1). Basement rocks along the eastern

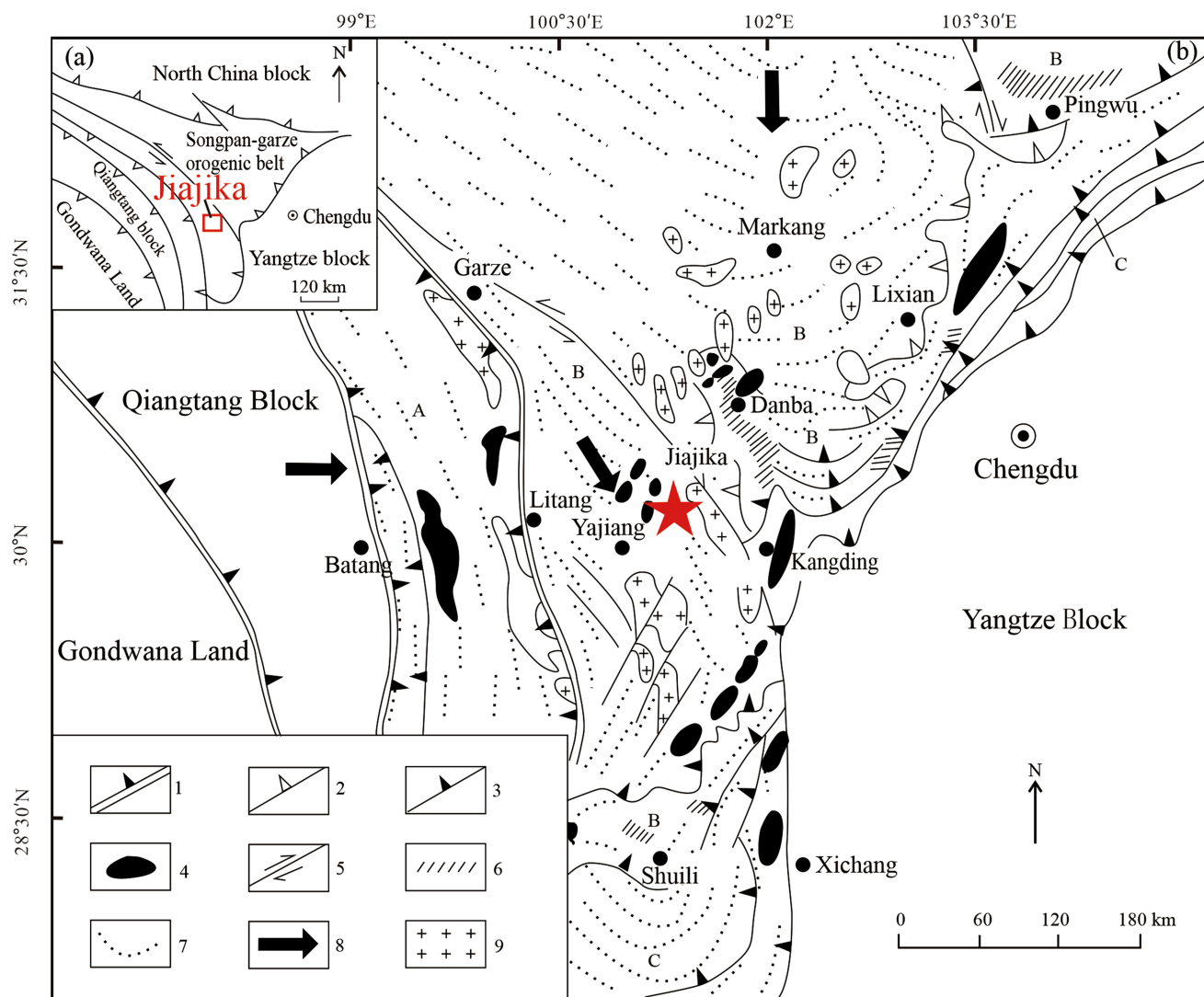


**Fig. 1** **a** Sketch of the Songpan–Garze orogenic belt and **b** simplified tectonic map of the Songpan–Garze orogenic belt (Modified after Xu et al. 1992; Fu et al. 2015; Hou et al. 2017; Li et al. 2020). 1. Ophiolitic mélange belt; 2. Detachment belt; 3. Thrust fault; 4. Dome-shaped deformed metamorphic body; 5. Strike-slip fault; 6. Outcrop area of a deep high-temperature ductile detachment shear zone; 7. Fold axis; 8. Vector of ductile slip; 9. Mesozoic granite. A—Yigou island-arc belt; B—Main part of the Songpan–Garze orogenic belt; C—Foreland thrust wedge

border of the SGOB comprise a Neoproterozoic crystalline complex (1.0–0.75 Ga; Roger et al. 2010; Dong and Santosh 2016) and overlying Late Triassic turbidites (Weislogel et al. 2010). The Songpan–Garze flysch complex, which occurs as a triangle-shaped fold belt between the North China, South China, and Qiangtang blocks, contains meta-turbidites of the Xikang Group (Fig. 1). The Xikang Group is composed of gray–black meta-felsic sandstones, meta-siltstone, sericite slate, silty slate, phyllite, schist, and minor limestone (Weislogel et al. 2010). The late Indosinian orogeny produced many NW- and NWW-trending folds, and the Jurassic Yanshan orogeny produced NE-striking reverse faults that formed under horizontal compression (Fig. 1). The SGOB contains large gneiss domes, including the Jiajika and Markang domes (De Sigoyer et al.

2014), which formed during the Late Triassic–Early Jurassic (Zhao et al. 2019).

Roger et al. (2004) proposed that collision among the Qiangtang, South China, and North China blocks during the Indosinian orogeny led to the development of a décollement between the basement and Triassic metasedimentary strata in the SGOB, resulting in crustal shortening and thickening. These processes might have led to decompression melting and indirect generation of rare-metal-bearing magma, leading ultimately to the crystallization of the pegmatite deposits in the SGOB (Li et al. 2019; Fei et al. 2020b). The deformation, magmatism, metamorphism, and mineralization in the eastern SGOB are temporally and spatially linked to exhumation during the Indosinian orogeny (Xu et al. 2020; Fei et al. 2020b).

The SGOB is a rare-metal pegmatite province that is similar to the Chinese Altay orogenic belt in terms of the number of pegmatites and economic rare-metal resources (Lv et al. 2012; Li et al. 2015a, b; Fei et al. 2020b). Some well-known pegmatite-type deposits have been discovered in the SGOB, including the Jiajika, Ke'eryin, Lijigou rare-metal deposits, and Danba rare-metal and muscovite deposits (Fig. 2).

Strata that crop out in the Jiajika deposit comprise mainly Triassic sandstones and shales of the Xikang Group, which were later transformed into biotite quartz schist, two-mica quartz schist, andalusite schist, and staurolite schist through regional and contact metamorphism under various temperature and pressure conditions (Li and Chou 2017). The deposit is cut by the NW–SE-trending dome-like Jiajika anticline, which in turn is cut by NW–SE-trending faults and X-shaped shear cracks. The Jiajika deposit contains north–south-trending two-mica granites that are exposed over an area of 5.5 km<sup>2</sup> (Fig. 3). Two-mica granites have been dated by the U–Pb zircon method, which yields ages of 206 to 223 Ma (Hao et al. 2015; Li et al. 2020). Pegmatite veins are found in fractures of the two-mica granite or fissures of the surrounding country rock (Fig. 4a), and are distributed in groups and bands (Fig. 3). According to the ore-bearing properties, the

pegmatites can be divided into two types: common pegmatites and spodumene pegmatites, the latter with metallogenic ages of 198 to 211 Ma as defined by LA-MC-ICP-MS cassiterite U–Pb dating (Dai et al. 2018a, 2019; Zhou et al. 2021). Previous studies have shown that the Jiajika granitic pegmatites were the final products of the extreme fractional crystallization of two-mica granitic magmas, and common pegmatites derived from early differentiation of the two-mica granitic magmas before they evolved into spodumene pegmatites during the late stage of magmatic differentiation (Zhang et al. 2021).

The Jiajika rare metal ore field, show the regional zonation of the pegmatite veins in the Jiajika area as follows: I-microcline pegmatite zone, II-microlime-albite pegmatite zone, III-albite pegmatite zone, IV-albite-spodumene pegmatite zone, V-albite-muscovite/lepidolite pegmatite zone. The granitic pegmatite veins radiate vertically and horizontally from the granite intrusion, and are divided into the following types based on the types of rare elements (with increasing distance from the intrusion) (Fig. 3): Be → Li → (Nb + Ta) → Cs or Be → Be-Nb-Ta → Li-Be-Nb-Ta → Li, Be, Nb, Ta, Cs, Sn zoning characteristics (Li 2006; Li and Chou 2017; Dai et al. 2019; Zhang et al. 2021; Fu et al. 2021). The main minerals are microcline, albite, quartz, and muscovite, along with

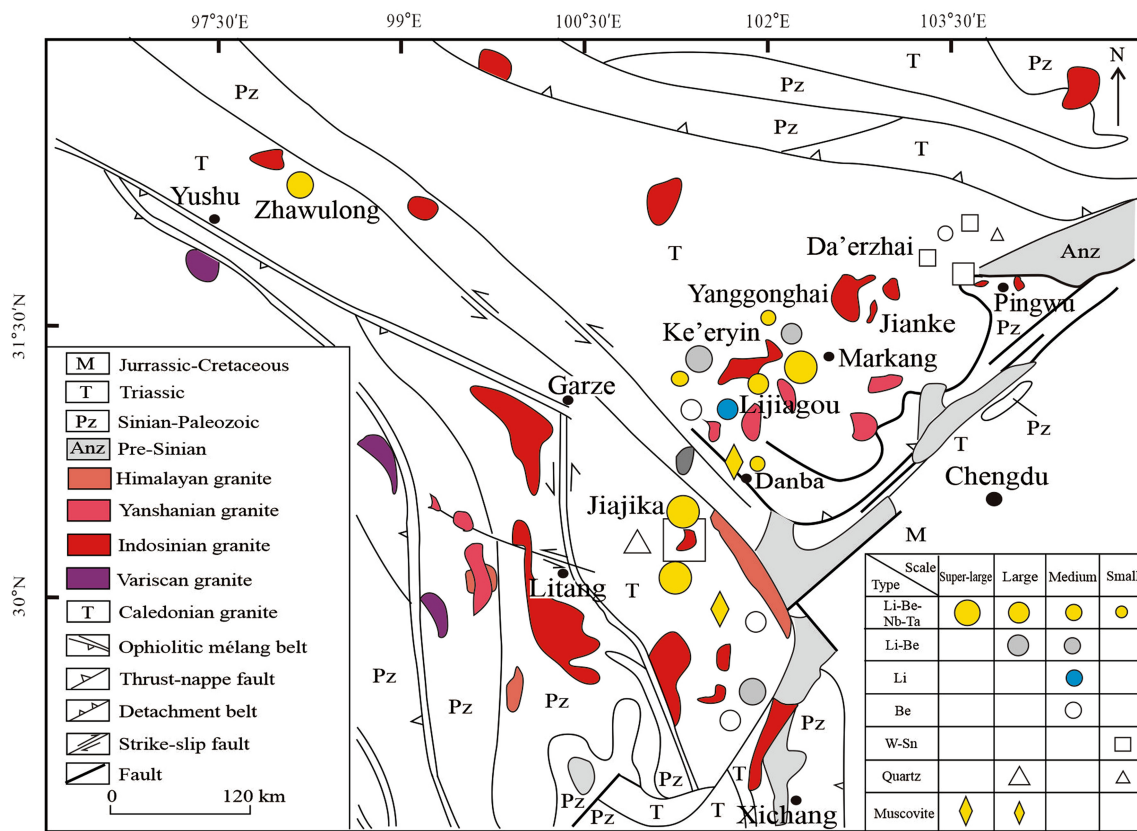


**Fig. 2** Distribution of rare-metal deposits in the Songpan–Garze orogenic belt (Modified after Li et al. 2014, 2015a, 2020; Dai et al. 2018a)

**Fig. 3** Simplified geological map of the Jiajika superlarge lithium deposit, Sichuan (Modified after Fu et al. 2015; Liang et al. 2016; Li and Chou 2016, 2017; Hou et al. 2017; Dai et al. 2018b, 2019; Li et al. 2020). 1. Two-mica granite; 2. Microcline-type pegmatite; 3. Microcline–albite-type pegmatite; 4. Albite-type pegmatite; 5. Albite–spodumene-type pegmatite; 6. Albite–lepidolite-type pegmatite; 7. Serial number of pegmatite vein; 8. Boundaries of different types of pegmatite; 9. Serial number of different types of pegmatite; 10. Newly identified ore veins and their serial number; 11. Sampling site and serial number for 2016; 12. Sampling site and serial number for 2017. I. Microcline-type pegmatite vein zone; II. Microcline–albite-type pegmatite vein zone; III. Albite-type pegmatite vein zone; IV. Albite–spodumene-type pegmatite vein zone; V. Albite–muscovite/lepidolite-type pegmatite vein zone

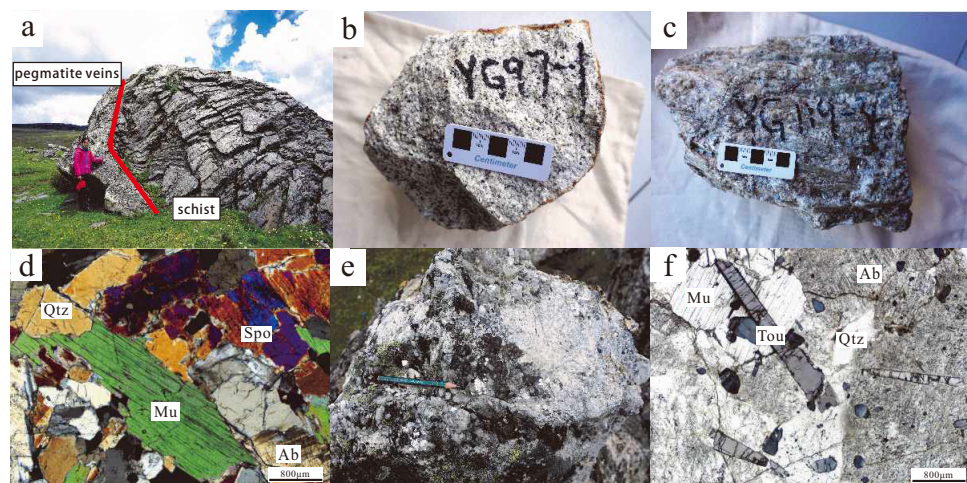
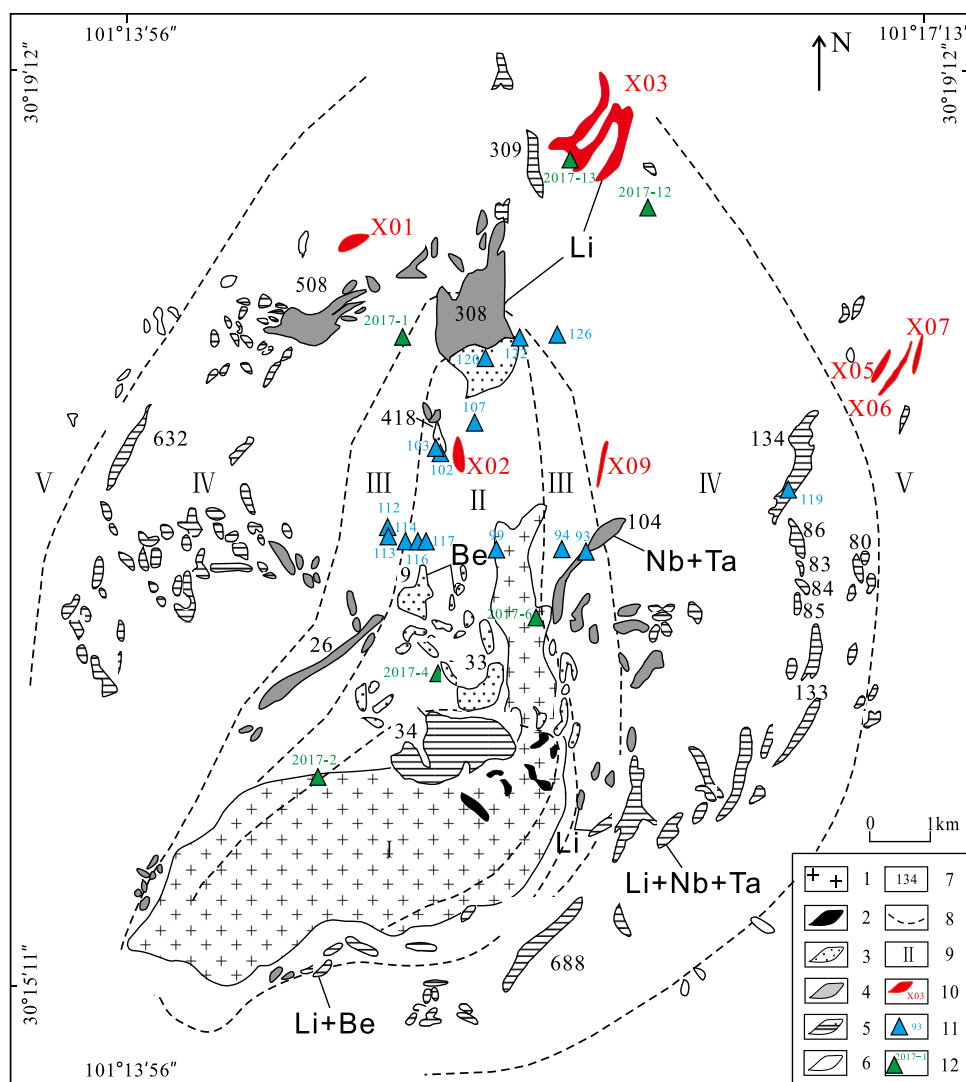


**Fig. 4** Typical field photographs and photomicrographs of rocks and minerals from the Jiajika superlarge lithium deposit, Sichuan (After Li et al. 2020). **a** Contact relationship between pegmatite veins and schist; **b** two-mica granite hand-specimen; **c** spodumene pegmatite hand-specimen; **d** spodumene pegmatite under cross-polarized light; **e** Common pegmatite hand-specimen; **f** Common pegmatite under plane-polarized light. Mu—Muscovite; Ab—Albite; Qtz—Quartz; Spo—Spodumene; Tou—Tourmaline

minerals that contain rare-metal elements, including spodumene, khlopinite, beryl, thorite, cyrtolite, and kymatolith (Wang et al. 2005).

Samples for analysis were collected from the different texture zones in the Jiajika rare metal ore field (Fig. 3). Spodumene pegmatites are distributed mainly in texture zones III–V, have a grayish-white color, pegmatic texture, and massive structure, and are composed mostly of quartz, albite, spodumene, and muscovite (Fig. 4c, d). Common pegmatites are distributed chiefly in texture zones I–II, show grayish black color and pegmatic texture, are massive and consist mainly of albite, quartz, tourmaline, and muscovite (Fig. 4e, f). Two-mica granites are also shown in Fig. 4b.

### 3 Analytical methods

#### 3.1 He–Ar isotope analyses

He and Ar isotopes were analyzed at the MNR Key Laboratory of Metallogeny and Mineral Assessment, Institute of Mineral Resources, Chinese Academy of Geological Sciences (CAGS), Beijing, China. Isotopes were measured using a Helix SFT mass spectrometer (Thermo Scientific) under high-vacuum conditions, with crushing and purification at  $n \times 10^{-9}$  mbar, and mass spectrometry at  $n \times 10^{-10}$  mbar. The sensitivity of the Helix SFT for He and Ar was  $> 2 \times 10^{-4}$  amps/Torr at 800  $\mu\text{A}$  and  $> 1 \times 10^{-3}$  amps/Torr at 200  $\mu\text{A}$ , respectively. The resolution of the Faraday cup was 400, and the resolution of the ion multiplier was better than 700, allowing the separation of  $^3\text{He}$  and  $^4\text{He}$ , and  $\text{HD} + \text{H}_2$  and  $^3\text{He}$ . Samples were degassed of labile volatiles and secondary fluid inclusions were discharged by heating under vacuum to 130–140 °C for 40 h. The detailed crushing and analytical procedures were described in Yang et al. (2016).

#### 3.2 H–O isotope analyses

H–O isotopes were analyzed using a MAT-253 mass spectrometer (Thermo Scientific) at the Analytical Laboratory of Beijing Research Institute of Uranium Geology, Beijing, China. Pure quartz, muscovite, and spodumene separates were prepared for H–O isotope analyses. Oxygen isotopic compositions were analyzed following the  $\text{BrF}_5$  method (Clayton and Mayeda 1963). Pure minerals were crushed to 200 mesh and reacted with  $\text{BrF}_5$  at 500–600 °C for 14 h to generate  $\text{O}_2$  that was reacted with graphite at 700 °C with a platinum catalyst to produce  $\text{CO}_2$ . The  $\text{CO}_2$  was then measured for O isotopes by mass spectrometry. The reproducibility for isotopically homogeneous standard quartz samples is about  $\pm 0.2\text{\textperthousand}$ .

For the H isotope analyses, water was released by heating the samples to  $\sim 500$  °C in an induction furnace. Samples were degassed of labile volatiles and secondary fluid inclusions were heated to 180–200 °C until the vacuum was less than  $10^{-1}$  Pa. Water was converted to  $\text{H}_2$  by passing over heated zinc powder at 400 °C, and  $\text{H}_2$  isotopes were analyzed by mass spectrometry. Analyses of standard water samples yielded a precision for  $\delta\text{D}$  of  $\pm 2\text{\textperthousand}$ .

## 4 Results

### 4.1 He and Ar isotopes

Table 1 lists the He and Ar isotopic compositions of quartz and spodumene from the Jiajika deposit. R/Ra ratios for common pegmatites ( $R: ^3\text{He}/^4\text{He}$  values of samples; Ra:  $1.4 \times 10^{-6}$ , the standard value of air) vary from 0.18 to 25.91 Ra (mean 7.73 Ra), and their  $^{40}\text{Ar}/^{36}\text{Ar}$  ratios range from 420.95 to 1430.51 (mean 749.79). R/Ra ratios for spodumene pegmatites vary from 0.18 to 6.76 Ra (mean 1.85 Ra), and their  $^{40}\text{Ar}/^{36}\text{Ar}$  ratios range from 402.13 to 1907.34 (mean 767.96).

### 4.2 H and O isotopes

Table 2 lists the H and O isotopic compositions of quartz, muscovite, and spodumene samples of this study, together with data from a previous study (Fei et al. 2017). The  $\delta^{18}\text{O}_{\text{H}_2\text{O}-\text{VSMOW}}$  values of common pegmatites range from 6.2‰ to 10.9‰, with a mean of 8.6‰, and their  $\delta\text{D}_{\text{V-SMOW}}$  values vary from  $-110\text{\textperthousand}$  to  $-72\text{\textperthousand}$ , with a mean of  $-85\text{\textperthousand}$ . The  $\delta^{18}\text{O}_{\text{H}_2\text{O}-\text{VSMOW}}$  values of spodumene pegmatites range from 5.3‰ to 13.2‰, with a mean of 9.1‰, and their  $\delta\text{D}_{\text{V-SMOW}}$  values vary from  $-115\text{\textperthousand}$  to  $-77\text{\textperthousand}$ , with a mean of  $-91\text{\textperthousand}$ .

## 5 Discussion

### 5.1 He–Ar isotopic compositions reveal the evolution of magmatic-hydrothermal fluids

As mentioned above, the He–Ar isotopes can be used as an ideal tracer for the crust and mantle contributions to the ore-forming processes (Turner et al. 1993a, b; Stuart et al. 1995; Wang et al. 2015; Li et al. 2018). There are four potential sources of He–Ar isotopes in hydrothermal fluids: (1) He and Ar in the atmosphere. Owing to the low He content in the atmosphere, there is no obvious influence on the composition of He isotopes in the hydrothermal fluids (Wen et al. 2016). However, the influence of Ar from the

**Table 1** He and Ar isotopic compositions and ratios of fluid inclusions trapped in quartz and spodumene from the Jiajika superlarge lithium deposit, Sichuan

Sample No	Mineral	<sup>3</sup> He	<sup>4</sup> He	<sup>36</sup> Ar	<sup>40</sup> Ar	<sup>40</sup> Ar*/ <sup>36</sup> Ar	<sup>3</sup> He'/ <sup>36</sup> Ar	<sup>40</sup> Ar*/ <sup>4</sup> He (Ra)	<sup>3</sup> He/ <sup>4</sup> He (Ra)	F/ <sup>4</sup> He	<sup>4</sup> He <sub>mantle</sub> (wt.%)
		10 <sup>-15</sup> cm <sup>3</sup> STP/g	10 <sup>-8</sup> cm <sup>3</sup> STP/g	10 <sup>-8</sup> cm <sup>3</sup> STP/g	10 <sup>-8</sup> cm <sup>3</sup> STP/g						
<i>Spodumene pegmatites</i>											
YG93-3	Quartz	77.65	2.08	0.0308	16.81	7.70	545.10	0.25	67.54	3.70	2.66
YG119-3	Quartz	10.36	4.21	0.0548	23.82	7.63	434.71	0.02	76.77	1.81	0.18
YG119-4	Quartz	61.13	14.73	0.0642	25.82	6.85	402.13	0.10	229.33	0.46	0.30
JJK2017-6-1	Quartz	225.50	15.85	0.0104	7.50	4.42	718.95	2.16	1518.60	0.28	1.02
*JJK2017-12-2	Quartz	221.77	2.34	0.0474	28.41	14.41	599.51	0.47	49.45	6.15	6.76
JJK2017-13-2	Spodumene	7032.18	2568.89	0.0535	102.00	86.20	1907.34	13.15	48,035.11	0.03	0.20
<i>Common pegmatites</i>											
YG99-2	Quartz	298.97	5.82	0.0868	122.20	96.55	1408.06	0.34	67.11	16.58	3.67
*YG102-1	Quartz	178.69	1.02	0.0310	23.43	14.26	754.83	0.58	32.76	14.02	12.55
*YG103-1	Quartz	164.26	0.55	0.0112	5.54	2.22	492.54	1.46	48.61	4.05	21.46
*YG113-3	Quartz	344.10	1.29	0.0438	33.25	20.30	758.63	0.79	29.43	15.74	19.06
*YG116-3	Quartz	449.24	5.49	0.0187	20.96	15.43	1118.67	2.40	292.74	2.81	5.85
YG117-3	Quartz	381.61	14.42	0.0351	18.56	8.18	528.41	1.09	410.65	0.57	1.89
YG120-2	Quartz	40.29	6.14	0.0217	14.02	7.60	645.61	0.19	282.69	1.24	0.47
*YG120-4	Quartz	101.46	0.56	0.0257	20.33	12.74	792.19	0.40	21.64	22.95	13.05
YG122-6	Quartz	27.33	4.49	0.0379	24.48	13.28	645.69	0.07	118.28	2.96	0.44
YG122-7	Quartz	18.49	7.29	0.4034	172.14	52.93	426.70	0.00	18.08	7.26	0.18
YG122-8	Quartz	49.41	0.86	0.0453	40.20	26.80	886.62	0.11	18.99	31.13	4.10
YG122-10	Quartz	27.78	3.98	0.0948	63.34	35.34	668.39	0.03	42.02	8.87	0.50
*JJK2017-1-2	Quartz	166.71	0.86	0.0152	21.75	17.25	1430.51	1.10	56.39	20.13	13.89
JJK2017-2-2	Quartz	600.42	9.17	0.0488	34.41	19.98	704.69	1.23	187.79	2.18	4.68
JJK2017-4-2	Quartz	374.16	27.38	0.0807	40.58	16.72	502.64	0.46	339.10	0.61	0.98
*YG102-2	Quartz core	515.08	4.67	0.0191	17.77	12.13	931.24	2.70	244.53	2.60	7.89
*YG103-2	Quartz core	414.38	2.41	0.0138	6.94	2.88	504.50	3.01	175.47	1.19	12.26
*YG112-3	Quartz core	415.35	1.14	0.0582	31.44	14.25	540.29	0.71	19.67	12.44	25.91
YG126-2	Quartz core	678.89	123.43	0.1038	70.68	40.01	681.05	0.65	1189.31	0.32	0.39
*YG102-3	Late quartz	574.05	2.22	0.0786	33.08	9.86	420.95	0.73	28.31	4.43	18.43
*YG107-4	Late quartz	424.77	2.61	0.0242	14.53	7.37	599.75	1.75	107.56	2.83	11.64

Table 1 continued

Sample No	Mineral	<sup>3</sup> He	<sup>4</sup> He	<sup>36</sup> Ar	<sup>40</sup> Ar	<sup>40</sup> Ar*	<sup>40</sup> Ar/ <sup>36</sup> Ar	<sup>3</sup> He/ <sup>36</sup> Ar	<sup>40</sup> Ar*/ <sup>4</sup> He (Ra)	<sup>3</sup> He/ <sup>4</sup> He (Ra)	<sup>4</sup> He/mantle (wt.%)
		10 <sup>-15</sup> cm <sup>3</sup> STP/g	10 <sup>-8</sup> cm <sup>3</sup> STP/g	10 <sup>-8</sup> cm <sup>3</sup> STP/g	10 <sup>-8</sup> cm <sup>3</sup> STP/g		10 <sup>-3</sup>				
*YG113-4	Late quartz	268.38	3.05	0.0275	19.10	10.96	693.73	0.97	110.92	3.59	6.28
YG114-3	Late quartz	840.34	61.34	0.0501	56.84	42.04	1134.89	1.68	1224.82	0.69	0.98
YG116-4	Late quartz	641.65	36.60	0.0904	82.22	55.49	909.02	0.71	404.64	1.52	1.25
*YG120-5	Late quartz	404.61	5.34	0.1126	63.64	30.37	565.24	0.36	47.45	5.68	5.41

<sup>40</sup>Ar\* is radiogenic <sup>40</sup>Ar, given all of the Ar come from the fluid inclusions, which can be expressed as <sup>40</sup>Ar\* = <sup>40</sup>Ar<sub>sample</sub> − 295.5 × <sup>36</sup>Ar<sub>sample</sub> (Ballentine and Burnard 2002); F<sup>4</sup>He values demonstrate enrichment of <sup>4</sup>He in the fluid relative to air, which can be illustrated as F<sup>4</sup>He = (<sup>4</sup>He/<sup>36</sup>Ar)<sub>sample</sub>/<sup>4</sup>He/<sup>36</sup>Ar<sub>air</sub>, where (<sup>4</sup>He/<sup>36</sup>Ar)<sub>air</sub> = 0.1727 (Stuart et al. 1995); <sup>4</sup>He/mantle values represent weight percent of mantle helium compared with crustal helium, which could be calculated as (<sup>4</sup>He/mantle/wt.%) = 100[(<sup>3</sup>He/<sup>4</sup>He)<sub>sample</sub> − (<sup>3</sup>He/<sup>4</sup>He)<sub>mantle</sub>] / [(<sup>3</sup>He/<sup>4</sup>He)<sub>sample</sub> − (<sup>3</sup>He/<sup>4</sup>He)<sub>mantle</sub>] (Anderson 2000)

\*Abnormal data

atmosphere on the hydrothermal fluids is uncertain (Marty et al. 1989; Stuart et al. 1994). (2) Air-saturated water (ASW), including seawater and sedimentary water. Under appropriate temperatures and pressures, air-saturated water is in equilibrium with the atmosphere and therefore has the same He–Ar isotope compositions: <sup>3</sup>He/<sup>4</sup>He = 1 Ra = 1.4 × 10<sup>-6</sup> and <sup>40</sup>Ar/<sup>36</sup>Ar = 295.5. However, the crust is enriched in U and Th, and <sup>4</sup>He generated by the decay of these elements will spread to shallow groundwater and surface water, causing the <sup>3</sup>He/<sup>4</sup>He ratio in the hydrothermal fluids to decrease, thereby showing the characteristics of reformed air-saturated water (Elliot et al. 1993; Stuart et al. 1994; Burnard et al. 1999; Ballentine and Burnard 2002). (3) Crust-derived fluids. The He–Ar isotopes in the crust originated mainly from radioactive decay, with <sup>3</sup>He/<sup>4</sup>He ≤ 0.1 Ra and <sup>40</sup>Ar/<sup>36</sup>Ar ≥ 45,000. Therefore, magmatic and metamorphic fluids of the crust have these isotopic compositions (Andrews 1985; Li et al. 2003). (4) Mantle-derived fluids. Mantle-derived fluids are usually rich in <sup>3</sup>He and poor in <sup>36</sup>Ar and have high <sup>3</sup>He/<sup>4</sup>He (7–9 Ra) and <sup>40</sup>Ar/<sup>36</sup>Ar (10,000–30,000) ratios for the MORB (Reid and Graham 1996; Burnard et al. 1999; Ozima and Podosek 2002; Xie et al. 2016).

Although some pegmatites have higher <sup>3</sup>He/<sup>4</sup>He ratios (Table 1; 5.41–25.91 Ra) than MORB, they have lower <sup>40</sup>Ar/<sup>36</sup>Ar (Table 1; 420.95–1430.51) ratios than MORB, which are significantly different from the mantle-derived fluids. These abnormally high <sup>3</sup>He/<sup>4</sup>He values might have been caused by the radioactive genesis of <sup>3</sup>He by lithium minerals through <sup>6</sup>Li (n, α) → <sup>3</sup>H (β) <sup>3</sup>He (e.g. Mamyrin and Tolstikhin 1984) and are excluded from the following discussion. The common pegmatites and spodumene pegmatites have <sup>3</sup>He/<sup>4</sup>He ratios that vary from 0.18 to 4.68 Ra (mean 1.62 Ra) and from 0.18 to 2.66 Ra (mean 0.87 Ra), respectively. These values are much higher than crustal values (0.01–0.05 Ra) but lower than mantle values (7–9 Ra; Kendrick et al. 2001), indicating that the fluids were shown a mixture of crust- and mantle-derived materials (Fig. 5a). It shows that the F<sup>4</sup>He values (105–278,142) in these samples are > 105 times larger than those in the atmosphere, suggesting a negligible contribution by atmospheric He. The <sup>3</sup>He/<sup>36</sup>Ar ratios (0–13.15) × 10<sup>-3</sup> in these samples are also much higher than those of atmosphere or air-saturated water (~ 5 × 10<sup>-8</sup>; Hu et al. 2009; Li et al. 2018), indicating that the He in the fluids that generated the Jiajika lithium deposit was non-atmospheric in origin. The ASW barely influences the He isotopic compositions of most fluids, given the low solubility of He in low-temperature aqueous fluids and the low abundance of atmospheric He (Burnard et al. 1999). Thus, the measured <sup>3</sup>He/<sup>4</sup>He ratios are inferred to have resulted from the mixing of crustal and mantle-derived materials He sources, and the contribution of mantle <sup>4</sup>He can be calculated as

**Table 2** Hydrogen and oxygen isotopic compositions of Jiajika superlarge lithium deposit and Lijiagou medium lithium deposit, Sichuan

Sample No	Mineral	$\delta^{18}\text{O}_{\text{V-SMOW}} (\text{\textperthousand})$	Th (°C)	$\delta^{18}\text{O}_{\text{H}_2\text{O-VSMOW}} (\text{\textperthousand})$	$\delta\text{D}_{\text{V-SMOW}} (\text{\textperthousand})$	References
<i>Spodumene pegmatites from the Jiajika deposit</i>						
YG93–3	Quartz	15.6	300	8.7	-115	This study
YG119–3	Quartz	15.8	300	8.9	-87	This study
YG119–4	Quartz	16.0	300	9.1	-96	This study
YG93–3	Muscovite	13.0	300	5.3	-84	This study
YG94–2	Muscovite	13.1	300	5.4	-77	This study
YG119–3	Muscovite	13.7	300	6.0	-80	This study
YG119–4	Muscovite	14.1	300	6.4	-82	This study
YG93–3	Spodumene	13.8	320	11.9	-77	This study
YG93–6	Spodumene	14.4	320	12.5	-110	This study
YG119–3	Spodumene	14.3	320	12.4	-99	This study
YG119–4	Spodumene	15.1	320	13.2	-90	This study
<i>Common pegmatites from the Jiajika deposit</i>						
YG99–2	Muscovite	14.3	300	6.6	-80	This study
YG102–1	Muscovite	14.7	300	7.0	-75	This study
YG103–1	Muscovite	14.1	300	6.4	-76	This study
YG103–2	Muscovite	15.0	300	7.3	-79	This study
YG113–3	Muscovite	14.4	300	6.7	-81	This study
YG116–3	Muscovite	14.7	300	7.0	-75	This study
YG117–3	Muscovite	14.5	300	6.8	-78	This study
YG120–2	Muscovite	14.9	300	7.2	-82	This study
YG120–4	Muscovite	13.9	300	6.2	-82	This study
YG122–7	Muscovite	13.9	300	6.2	-83	This study
YG122–8	Muscovite	14.5	300	6.8	-82	This study
YG122–10	Muscovite	14.3	300	6.6	-81	This study
YG99–2	Quartz	16.2	300	9.3	-89	This study
YG102–1	Quartz	17.2	300	10.3	-106	This study
YG103–1	Quartz	16.1	300	9.2	-90	This study
YG113–3	Quartz	17.3	300	10.4	-72	This study
YG116–3	Quartz	17.1	300	10.2	-74	This study
YG117–3	Quartz	15.5	300	8.6	-74	This study
YG120–2	Quartz	16.9	300	10.0	-84	This study
YG120–4	Quartz	17.3	300	10.4	-98	This study
YG122–6	Quartz	16.4	300	9.5	-88	This study
YG122–7	Quartz	16.8	300	9.9	-84	This study
YG122–8	Quartz	16.6	300	9.7	-100	This study
YG122–10	Quartz	16.5	300	9.6	-84	This study
YG102–2	Quartz core	16.4	320	10.2	-99	This study
YG103–2	Quartz core	16.3	320	10.1	-91	This study
YG112–3	Quartz core	17.1	320	10.9	-79	This study
YG126–2	Quartz core	15.7	320	9.5	-89	This study
YG102–3	Late quartz	16.2	280	8.6	-88	This study
YG107–4	Late quartz	16.4	280	8.7	-83	This study
YG113–4	Late quartz	17.2	280	9.5	-110	This study
YG114–3	Late quartz	17.0	280	9.3	-79	This study
YG116–4	Late quartz	16.1	280	8.4	-82	This study
YG120–5	Late quartz	16.6	280	8.9	-100	This study
<i>Lijiagou deposit</i>						

**Table 2** continued

Sample No	Mineral	$\delta^{18}\text{O}_{\text{V-SMOW}} (\text{\textperthousand})$	Th (°C)	$\delta^{18}\text{O}_{\text{H}_2\text{O-VSMOW}} (\text{\textperthousand})$	$\delta\text{D}_{\text{V-SMOW}} (\text{\textperthousand})$	References
LPD1H2	Spodumene	11.1	220	-0.2	-62	Fei et al. (2017)
LPD2H2	Spodumene	14.0	220	2.7	-69	Fei et al. (2017)
LPD3H2	Spodumene	13.0	220	1.7	-79	Fei et al. (2017)
LPD4H2	Spodumene	11.7	220	0.4	-86	Fei et al. (2017)
LPD1H2	Quartz	14.9	237	5.3	-59	Fei et al. (2017)
LPD2H2	Quartz	14.8	213	3.9	-66	Fei et al. (2017)
LPD3H2	Quartz	15.8	225	5.6	-65	Fei et al. (2017)
LPD4H2	Quartz	15.1	225	4.9	-74	Fei et al. (2017)
LKH3	Quartz	13.8	257	5.2	-77	Fei et al. (2017)
LYH1	Quartz	15.8	257	7.2	-75	Fei et al. (2017)

The  $\delta^{18}\text{O}_{\text{H}_2\text{O-VSMOW}}$  values of fluid inclusions in the quartz, muscovite and spodumene were calculated according to the equations of  $1000\ln a_{\text{quartz-water}} = 3.38 \times 10^6/T^2 - 3.40$  (Clayton et al. 1972),  $1000\ln a_{\text{muscovite-water}} = 3.20 \times 10^6/T^2 - 2.00$  (O'Neil et al. 1969), and  $1000\ln a_{\text{spodumene-water}} = 4.17 \times 10^6/T^2 - 7.19 \times 10^3/T + 2.18$  (Zheng 1993), respectively. Th (°C) for the Jiajika deposit was provided by Dr. Xiongxin, from the MNR Key Laboratory of Metallogeny and Mineral Assessment, Institute of Mineral Resources, Chinese Academy of Geological Sciences

follows:  ${}^4\text{He}_{\text{mantle}} (\text{wt.\%}) = 100 \times [({}^3\text{He}/{}^4\text{He})_{\text{sample}} - ({}^3\text{H}/{}^4\text{He})_{\text{crust}}]/[({}^3\text{He}/{}^4\text{He})_{\text{mantle}} - ({}^3\text{He}/{}^4\text{He})_{\text{crust}}]$ , where  $({}^3\text{H}/{}^4\text{He})_{\text{crust}} = 0.01 \text{ Ra}$ ,  $({}^3\text{He}/{}^4\text{He})_{\text{mantle}} = 6.00 \text{ Ra}$  (Anderson 2000; Kendrick et al. 2001). The calculations show that the percentage of mantle-derived He in the common pegmatites ranges from 2.86% to 77.91%, with a mean of 26.98%; whereas that in the spodumene pegmatites ranges from 2.77% to 44.29%, with a mean of 14.35%. The mantle component indicates that the hydrothermal fluids in the Jiajika deposit were dominated by crust-derived materials, with a relatively small contribution from mantle-derived materials; as mineralization progressed from common pegmatites to spodumene pegmatites, the proportion of crust-derived materials gradually increased (Fig. 5). The addition of mantle-derived materials in ore-forming fluids is likely due to the existence of ancient crust with mantle-derived materials, such as Proterozoic immature crust or Precambrian basement (Liu et al. 2021; Luo et al. 2022). The  $\varepsilon_{\text{Hf}}(t)$  values of the pegmatites in the Jiajika deposit range from  $-10.3$  to  $-5.5$ , and their Hf model ages ( $T_{\text{DM}}^{\text{C}}$ ) are in the range of 1.6–1.66 Ga (Li et al. 2020). The negative  $\varepsilon_{\text{Hf}}(t)$  and older  $T_{\text{DM}}^{\text{C}}$  values were interpreted to derive from the partial melting of the Triassic metasedimentary rocks from the SGOB (Yan et al. 2020).

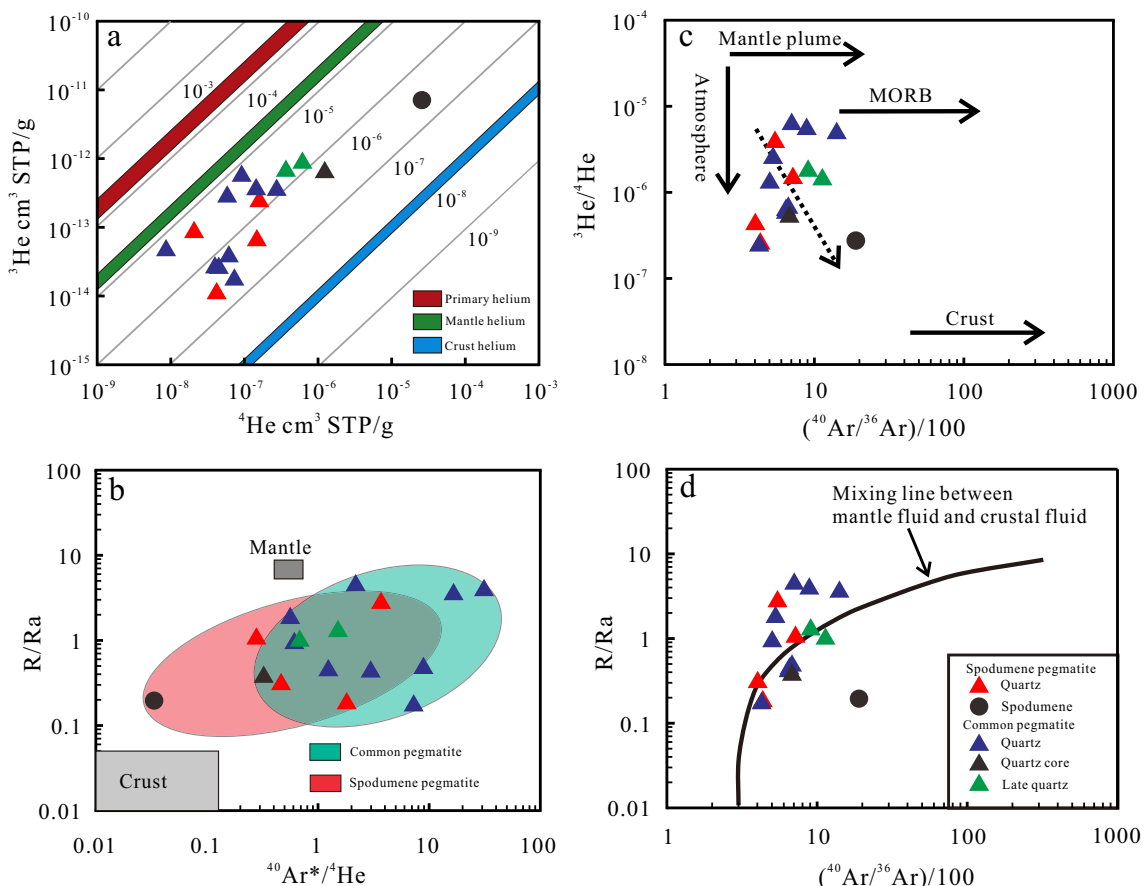
Common pegmatites and spodumene pegmatites yield  ${}^{40}\text{Ar}/{}^{36}\text{Ar}$  ratios of 426.70–1408.06 (mean 761.81) and 402.13–1907.34 (mean 801.65), respectively. Ratios of  ${}^{40}\text{Ar}/{}^{36}\text{Ar}$  and  ${}^3\text{He}/{}^4\text{He}$  suggest that the hydrothermal fluids might have resulted from the mixing of different proportions of crust- and mantle-derived materials (Fig. 5c). On R/Ra versus  ${}^{40}\text{Ar}/{}^{36}\text{Ar}/100$  and R/Ra versus  ${}^{40}\text{Ar}^*/{}^4\text{He}$

diagram (Fig. 5b, d), data for the Jiajika lithium deposit fall between the fields of crust-derived and mantle-derived materials, which is consistent with the He isotope data. In general, the radiogenic  ${}^{40}\text{Ar}$  ( ${}^{40}\text{Ar}^*$ ) easily diffused into groundwater and pore fluids, so the crust-derived materials trapped in the fluid inclusions might be a mixture of ASW argon and radiogenic  ${}^{40}\text{Ar}$  (Turner et al. 1993a, b; Xie et al. 2016). The percentage of  ${}^{40}\text{Ar}^*$  can be calculated using  ${}^{40}\text{Ar}^* = {}^{40}\text{Ar}_{\text{sample}} - 295.5 \times {}^{36}\text{Ar}_{\text{sample}}$  (Ballentine and Burnard 2002). Results of the calculations show that the percentage of  ${}^{40}\text{Ar}^*$  for common pegmatites ranges from 7.6% to 96.55%, with a mean of 34.58%, and those of Ar is 3.45% to 92.4%, with a mean of 65.42%. The percentage of  ${}^{40}\text{Ar}^*$  for spodumene pegmatites ranges from 4.42% to 86.2%, with a mean of 22.56%, and those of Ar is 13.8% to 95.58%, with a mean of 77.44%. These values indicate that the Ar in the hydrothermal fluids was derived mainly from meteoric water. On R/Ra versus  ${}^{40}\text{Ar}/{}^{36}\text{Ar}$  diagram (Fig. 6), some samples are around the ASW endmember, supporting this inference.

All of these He–Ar isotopic signatures suggest that the hydrothermal fluids in the Jiajika deposit were dominated by crust-derived materials and have more crustal components than those of mantle-derived materials and significant involvement of meteoric water in the fluid system.

## 5.2 H–O isotopic compositions reveal the evolution of magmatic-hydrothermal fluids

Isotopes of H and O provide clues to the nature and evolution of ore fluids (Chen et al. 2009; Hou et al. 2009;



**Fig. 5** Diagrams of He–Ar isotopes of fluid inclusions from the Jiajika superlarge lithium deposit, Sichuan. **a** Plot of  ${}^3\text{He}$  versus  ${}^4\text{He}$  (Base map after Mamyrin and Tolstikhin 1984); **b** Plot of  $R/R_a$  versus  ${}^{40}\text{Ar}^*/{}^4\text{He}$  (Base map after Hu et al. 1997); **c** Plot of  ${}^3\text{He}/{}^4\text{He}$  versus  $({}^{40}\text{Ar}/{}^{36}\text{Ar})/100$  (Base map after Wang et al. 2002); **d** Plot of  $R/R_a$  versus  $({}^{40}\text{Ar}/{}^{36}\text{Ar})/100$  (Base map after Hu et al. 1999)

Wang et al. 2018a, b). In this study, the calculated  $\delta^{18}\text{O}_{\text{H}_2\text{O}-\text{VSMOW}}$  and  $\delta D_{\text{V-SMOW}}$  data of spodumene pegmatites are 5.3‰ to 13.2‰, with a mean of 9.1‰, and –115‰ to –77‰, with a mean of –91‰, respectively, which are plotted in the area between the meteoric water line and the primary magmatic water field but near the magmatic water field in the  $\delta\text{D}-\delta^{18}\text{O}$  diagram (Fig. 7). H–O isotopic compositions show that the primary ore-forming fluids dominantly originated from magma water, which is consistent with the previous Li isotope results. It is considered that the ore-forming fluid is derived from the original magma (Zhang et al. 2021). In addition, the quartz and mica samples mainly fall near the magmatic water region, but the spodumene samples show higher  $\delta^{18}\text{O}_{\text{H}_2\text{O}-\text{VSMOW}}$  values outside the magmatic water region. This might be due to the addition of metamorphic fluid ( $\delta\text{D} = -20\text{\textperthousand}$  to  $-65\text{\textperthousand}$ ;  $\delta^{18}\text{O} = 4\text{\textperthousand}$  to  $20\text{\textperthousand}$ ; Taylor 1974), and indicates that the formation of lithium deposits is closely related to metasedimentary rocks in the region. Notably, the  $\delta D_{\text{V-SMOW}}$  values of all pegmatites are relatively lower than those of the typical magmatic water, and could be interpreted as the participation of paleometeoric

water in the continuous degassing of the parent magma (Fig. 7; Chelle-Michou et al. 2017; Sun et al. 2017; Wang et al. 2018a, b; Liu et al. 2020a). Extensive studies have shown that D preferentially partitions into the vapor phase relative to H during fluid boiling, and the value of  $\delta D_{\text{V-SMOW}}$  in the residual fluid decreases by about 28‰ while scarcely changing the  $\delta^{18}\text{O}_{\text{H}_2\text{O}-\text{VSMOW}}$  (Shmulovich et al. 1999; Driesner and Seward 2000). Hence, we conclude that the large variations of  $\delta D_{\text{V-SMOW}}$  of fluid inclusions in quartz and spodumene were caused by meteoric water and fluid boiling. Moreover, the  $\delta D_{\text{V-SMOW}}$  deficit of spodumene pegmatites is stronger than common pegmatites, and the variation range is wider (Fig. 7). These values imply that the ore-forming fluids originated from magmatic water gradually mixing with more meteoric water in the late stage of the magmatic evolution.

Compared with the Lijiagou deposit (Fig. 7), a greater proportion of meteoric water was added to the ore-forming fluids during mineralization in the Jiajika deposit, which might have contributed to the larger resources of the Jiajika deposit.

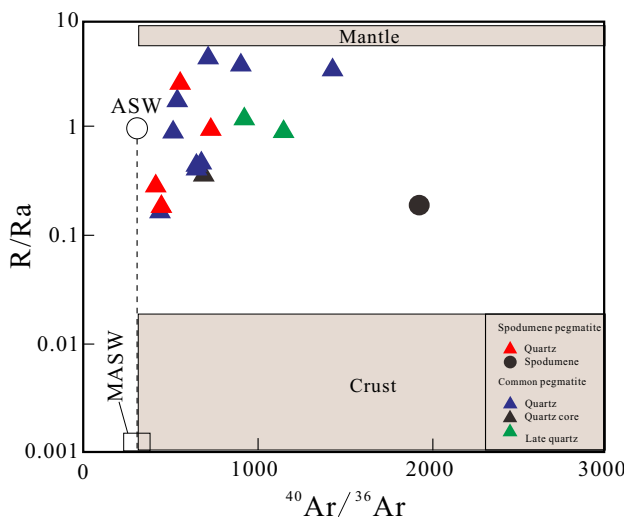


**Fig. 6** Plot of  ${}^3\text{He}/{}^4\text{He}$  ( $\text{R}/\text{Ra}$ ) versus  ${}^{40}\text{Ar}/{}^{36}\text{Ar}$  ratios of fluids inclusions from the Jiajika superlarge lithium deposit, Sichuan (Base map from Zhang et al. 2018). ASW—Air-saturated water; MASW—Modified air-saturated water

### 5.3 Mineralization processes of the Jiajika superlarge lithium deposit

Despite extensive studies on pegmatites over several decades, their petrogenesis remains controversial, it is commonly considered that pegmatite is the product of the crystallization differentiation of granitic magmas, which leads to the enrichment of rare metals in residual magmas (Černý and Ercit 2005; London 2008; Deveaud et al. 2015; Roda-Robles et al. 2018; Yan et al. 2020; Wang et al. 2020). The newly published major elements, trace elements, rare earth elements (REEs), and Pb–Sr–Nd–Li isotopes in the Jiajika deposit indicate that pegmatites are genetically associated with the two-mica granites and are products of the extreme fractional crystallization of two-mica granite-forming magma (Li et al. 2020; Zhang et al. 2021), whereas two-mica granites were generated by partial melting of schists and slates (Li et al. 2020). The mineralization processes of the Jiajika lithium deposit in western Sichuan have been described as primary enrichment during the sedimentation process (sedimentation, metamorphism, deep burying, and remelting), secondary enrichment during the formation of granite and tertiary enrichment during the formation of pegmatite (crystallization differentiation of granite-forming magma, fluid exsolution) (Li et al. 2020; Zhang et al. 2021).

The He–Ar isotope compositions suggest that the hydrothermal fluids have mixed characteristics of those derived from both crust- and mantle-derived materials and that the proportion of crust-derived materials in spodumene pegmatites increases significantly in the late stage of the magmatic evolution (Figs. 5, 6). The H–O isotope data

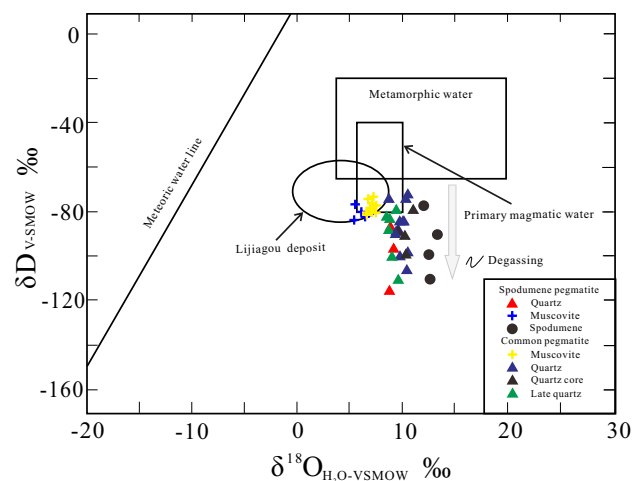


**Fig. 7**  $\delta\text{D}-\delta{}^{18}\text{O}$  diagram for hydrothermal fluids from the Jiajika superlarge lithium deposit, Sichuan (Base map from Taylor 1974)

indicate that the ore-forming fluids came from magmatic water gradually mixing with more meteoric water in the late stage of the magmatic evolution (Fig. 7). On the  $\delta{}^{18}\text{O}$  versus  $\delta\text{D}$  diagram (Fig. 7), fluid inclusions in muscovite, quartz and spodumene show different H–O isotopic compositions, indicating that minerals in the ore-forming process have different formation conditions. Notably, the  $\delta{}^{18}\text{O}$  values from the spodumene are slightly higher than those of the primary magmatic waters (Fig. 7). In addition, the fluids inclusions of spodumenes have characteristics of high temperature (Fig. 8;  $22.86 \times 10^{-10} \text{ cm}^3 \text{ STP/J}$ ) and high metal content (e.g., Li, Be, Cs, Rb; Deng et al. 2022; Wang et al. 2022), and their  ${}^3\text{He}/\text{Q}$  estimates are even much higher than those of hydrothermal fluids from mid-oceanic ridges ( $0.1\text{--}0.2 \times 10^{-12} \text{ cm}^3 \text{ STP/J}$ ; Lupton et al. 1989; Baker and Lupton 1990), which is similar to typical exsolved magmatic fluids (Audébat et al. 2008). It is consistent with the conclusion of the Li isotope, indicating that fluid exsolution occurred during the separation of melt and fluid at a late stage of the magmatic evolution (Zhang et al. 2021).

Based on these and existing data, we propose the following processes of mineralization of the Jiajika superlarge lithium deposit. Geochronological studies suggest that the Jiajika granite- and pegmatite-type Li deposit was formed during the Late Triassic between 181 and 216 Ma, which is a relatively quiet period after the strong Indosinian activities (Zhang et al. 2021). During the late Indosinian, subduction and collision between the Qiangtang, South China, and North China blocks led to crustal shortening and thickening, resulting in regional and contact metamorphism under various temperature and pressure conditions (Roger et al. 2004). These processes might have caused Triassic sandstones and shales of the Xikang Group to be transformed into biotite quartz schist, two-mica quartz schist,

andalusite schist, and staurolite schist (Li et al. 2019, 2020; Yan et al. 2020). Li and other rare metal elements, including Be, Rb, Cs, Nb, and Ta, were enriched during thermal metamorphism (Li et al. 2020; Wang et al. 2020). For example, the lithium content of cordierite schist can be 10 times as much as ordinary schist (Wang et al. 2020). At this time, these orogenic movements could also cause the melting of the ancient crust with mantle-derived materials and the formation of Li-bearing silicate magma. This Li-bearing magma ascended, undergoing fractional crystallization and fluid exsolution. The ore-forming fluid exsolved from the magma and moved upwards or outwards through the secondary fractures generated by the formation of the dome (Li et al. 2007a). At the late crystallization stage, the fluid exsolution can produce H<sub>2</sub>O-poor silicate-rich and H<sub>2</sub>O-rich silicate-poor pegmatite systems (Zhang et al. 2021). The H<sub>2</sub>O-poor silicate-rich pegmatite magmas migrated only short distances, filling fractures and gaps within the host metamorphic strata with weak metasomatism and inconspicuous addition of meteoric water, forming common pegmatite veins (Zhai et al. 2011; Thomas et al. 2012). In contrast, the H<sub>2</sub>O-rich silicate-poor granitic pegmatite magmas over longer distances within the fractures in host rocks enabled the replacement of some early-formed minerals and mineralizing elements (e.g., Li, Be, Nb, Ta, and other rare elements) in the host rocks and the obvious addition of meteoric water, forming spodumene pegmatite veins (Zhai et al. 2011; Thomas et al. 2012).

The obtained He–Ar–H–O isotope data from the Jiaka lithium deposit suggest that the ore fluids are most likely derived from the crust and modified due to mixing and dilution with meteoric waters. The lithium and other rare metals, i.e., beryllium, and probably niobium and tantalum originate from both local sedimentary sources, which are further enriched through geological processes such as metamorphism, remelting, fractional crystallization, and fluid exsolution. The magmatic fluid exsolved from the late stage of melt is likely to represent a supercritical fluid, which is an important carrier of lithium. Therefore, the continuing addition of meteoric water and fluid exsolution during the formation of pegmatite are the key to the form of Li ore bodies and led to the enrichment of Li in the altered surrounding rocks (Triassic sedimentary rocks of the Xikang Group).

## 6 Conclusions

We performed an integrated analysis of He–Ar–H–O isotopes to trace the evolution of magmatic-hydrothermal fluids and determine the processes of mineralization of the Jiajika superlarge lithium deposit in western Sichuan Province, China. Our main conclusions are as follows.

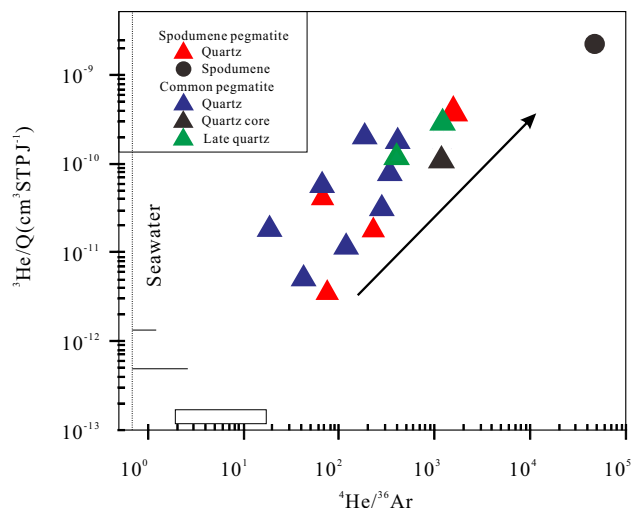


**Fig. 8**  ${}^3\text{He}/\text{Q}$  versus  ${}^4\text{He}/{}^{36}\text{Ar}$  for Spodumene and Quartz from the Jiajika superlarge lithium deposit. The calculation formula is  ${}^3\text{He}/\text{Q} = {}^3\text{He}/{}^{36}\text{Ar} \times [{}^{36}\text{Ar}]_{\text{MASW}}/(C_P \theta)$  from Turner and Stuart (1992) and Burnard et al. (1999), where  $[{}^{36}\text{Ar}]_{\text{MASW}}$  is the concentration of  ${}^{36}\text{Ar}$  in MASW ( $7.65 \times 10^{-7} \text{ cm}^3 \text{ STP/g}$ ),  $C_P$  is the specific heat of MASW ( $4.4 \text{ JK}^{-1} \text{ g}^{-1}$ ) and  $\theta$  is the temperature increase of the cold fluid ( $^\circ\text{C}$ ). Solid horizontal lines = range in  ${}^4\text{He}/{}^{36}\text{Ar}$  of EPR (East Pacific Rise) vent fluids and plumes (Lupton et al. 1989, 1995); Box = Lucky Strike vent fluids (Jean-Baptiste et al. 1998)

- (1) He and Ar isotope compositions suggest that both mantle- and crust-derived materials were involved in the Li mineralization and that the proportion of crust-derived materials in spodumene pegmatites increases significantly in the late stage of the magmatic evolution.
- (2) The  $\delta D_{\text{V-SMOW}}$  and  $\delta^{18}\text{O}_{\text{H}_2\text{O-VSMOW}}$  values indicate that the ore-forming fluids derived from magmatic water gradually mixed with more meteoric water in the late stage of the magmatic evolution.
- (3) Detailed mineralization processes for the Jiajika lithium deposit include sedimentation, metamorphism, deep burial, remelting, fractional crystallization, and fluid exsolution. The ore-forming metals are mainly derived from the upper continental crust with a minor contribution from the mantle. The fluid exsolution and addition of meteoric water during the formation of pegmatite contributed to the formation of the Jiajika lithium deposit.

**Acknowledgements** We thank two anonymous reviewers for their insightful and critical comments and suggestions, which significantly improved the manuscript. The careful and efficient editorial handling by Managing Editor Binbin Wang is greatly appreciated. This research was financially supported by grants from the National Key Research and Development Project of China (2021YFC2901903 and 2017YFC0602705), the Jiangxi Province (2020101003), and the East China University of Technology (1410000874).

**Author contributions** TIAN Shihong, WANG Denghong, LI Xianfang, FU Xiaofang, HAO Xuefeng and ZHANG Yujie collected the samples in the field; LI Xianfang, ZHANG Yujie and HOU Kejun performed the experiments; LIU Tao, TIAN Shihong and WANG Hai contributed to discussions, interpretation of results and manuscript writing. Correspondence and requests for materials should be addressed to LIU Tao (liutao1370693421@163.com) or TIAN Shihong (tshhong@ecut.edu.cn).

## Declarations

**Conflict of interest** The authors declare that the research was conducted in the absence of any commercial or financial relationships that could be construed as a potential conflict of interest.

## References

- Anderson DL (2000) The statistics and distribution of helium in the mantle. *Int Geol Rev* 42(4):289–311. <https://doi.org/10.1080/00206810009465084>
- Andrews JN (1985) The isotopic composition of radiogenic helium and its use to study groundwater movement in confined aquifers. *Chem Geol* 49(1–3):339–351. [https://doi.org/10.1016/0009-2541\(85\)90166-4](https://doi.org/10.1016/0009-2541(85)90166-4)
- Audétat A, Pettke T, Heinrich CA, Bodnar RJ (2008) The composition of magmatic-hydrothermal fluids in barren and mineralized intrusions. *Econ Geol* 103:877–908. <https://doi.org/10.2113/gsecongeo.103.5.877>
- Baker E, Lupton J (1990) Changes in submarine hydrothermal  ${}^3\text{He}$ /heat ratios as an indicator of magmatic/tectonic activity. *Nature* 346(6284):556–558. <https://doi.org/10.1038/346556a0>
- Ballentine CJ, Burnard PG (2002) Production, release and transport of noble gases in the continental crust. *Rev Miner Geochem* 47(1):481–538. <https://doi.org/10.2138/rmg.2002.47.12>
- Barros R, Menute JF (2016) The origin of spodumene pegmatites associated with the Leinster granite in Southeast Ireland. *Can Miner* 54(4):847–862. <https://doi.org/10.3749/canmin.1600027>
- Burnard PG, Hu RZ, Turner G, Bi XW (1999) Mantle, crustal and atmosphere noble gases in Ailaoshan gold deposit, Yunnan province China. *Geochim Cosmochim Acta* 63(10):1595–1604. [https://doi.org/10.1016/S0016-7037\(99\)00108-8](https://doi.org/10.1016/S0016-7037(99)00108-8)
- Černý P, Ercit TS (2005) The classification of granitic pegmatites revisited. *Can Miner* 43(6):2005–2026. <https://doi.org/10.2113/gscanmin.43.6.2005>
- Chelle-Michou C, Rottier B, Caricchi L, Simpson G (2017) Tempo of magma degassing and the genesis of porphyry copper deposits. *Sci Rep* 7(1):40566. <https://doi.org/10.1038/srep40566>
- Chen YJ, Pirajno F, Li N, Guo DS, Lai Y (2009) Isotope systematic and fluid inclusion studies of the Qiyugou breccias pipe-hosted gold deposit, Qinling Orogen, Henan province, China: implications for ore genesis. *Ore Geol Rev* 35(2):245–261. <https://doi.org/10.1016/j.oregeorev.2008.11.003>
- Chen XC, Zhao CH, Zhu JJ, Wang XS, Cui T (2018) He, Ar, and S isotopic constraints on the relationship between A-type granites and tin mineralization: a case study of tin deposits in the Tengchong-Lianghe tin belt, southwest China. *Ore Geol Rev* 92:416–429. <https://doi.org/10.1016/j.oregeorev.2017.11.032>
- Clayton RN, Mayeda TK (1963) The use of bromine and pentafluoride in the extraction of oxygen from oxide and silicates for isotopes analysis. *Geochim Cosmochim Acta* 27(1):43–52. [https://doi.org/10.1016/0016-7037\(63\)90071-1](https://doi.org/10.1016/0016-7037(63)90071-1)
- Clayton RN, O' Neil JR, Mayeda TK (1972) Oxygen isotope exchange between quartz and water. *J Geophys Res* 77(17):3057–3067. <https://doi.org/10.1029/JB077i017p03057>
- Dai HZ, Wang DH, Liu LJ, Yu Y, Dai JJ (2018a) A study on the emerald in the Jiajika rare metal mining area, Sichuan Province China. *Acta Mineral Sin* 38(2):135–141 (in Chinese with English abstract)
- Dai HZ, Wang DH, Liu LJ, Yu Y, Dai JJ, Fu XF (2018b) Geochronology, geochemistry and their geological significances of No. 308 pegmatite vein in the Jiajika deposit, western Sichuan China. *Earth Sci* 43(10):3664–3681 (in Chinese with English abstract)
- Dai HZ, Wang DH, Liu LJ, Yu Y, Dai JJ (2019) Geochronology and Geochemistry of Li(Be)-Bearing Granitic Pegmatites from the Jiajika Superlarge Li-Polymetallic Deposit in Western Sichuan China. *J Earth Sci* 30(4):707–727. <https://doi.org/10.1007/s12583-019-1011-9>
- De Sigoyer J, Vanderhaeghe O, Duchene S (2014) Generation and emplacement of Triassic granitoids within the Songpan-Garze accretionary-orogenic wedge in a context of slab retreat accommodated by tear faulting, Eastern Tibetan Plateau China. *J Asian Earth Sci* 88:192–216. <https://doi.org/10.1016/j.jseaes.2014.01.010>
- Deng JY, Li JK, Zhang DH, Chou IM, Yan QG, Xiong X (2022) Origin of pegmatitic melts from granitic magmas in the formation of the Jiajika lithium deposit in the eastern Tibetan Plateau. *J Asian Earth Sci*. <https://doi.org/10.1016/j.jseaes.2022.105147>
- Deveaud S, Millot R, Villaro A (2015) The genesis of LCT-type granitic pegmatites, as illustrated by lithium isotopes in micas. *Chem Geol* 411:97–111. <https://doi.org/10.1016/j.chemgeo.2015.06.029>
- Dill HG (2015) Pegmatites and aplites: their genetic and applied ore geology. *Ore Geol Rev* 69:417–561. <https://doi.org/10.1016/j.oregeorev.2015.02.022>
- Dill HG (2018) Geology and chemistry of Variscan-type pegmatite systems (SE Germany) with special reference to structural and chemical pattern recognition of felsic mobile components in the crust. *Ore Geol Rev* 92:205–239. <https://doi.org/10.1016/j.oregeorev.2017.11.016>
- Dong YP, Santosh M (2016) Tectonic architecture and multiple orogeny of the Qinling Orogenic Belt Central China. *Gondwana Res* 29(1):1–40. <https://doi.org/10.1016/j.gr.2015.06.009>
- Driesner T, Seward T (2000) Experimental and simulation study of salt effects and pressure/density effects on oxygen and hydrogen stable isotope liquid-vapor fractionation for 4–5 molal aqueous NaCl and KCl solutions to 400°C. *Geochim Cosmochim Acta* 64(10):1773–1784. [https://doi.org/10.1016/S0016-7037\(99\)00435-4](https://doi.org/10.1016/S0016-7037(99)00435-4)
- Elliot T, Ballentine CJ, O' nions RK, Ricchiuto T (1993) Carbon, helium, neon and argon isotopes in a Po basin (northern Italy) natural gas field. *Chem Geol* 106(3):429–440. [https://doi.org/10.1016/0009-2541\(93\)90042-H](https://doi.org/10.1016/0009-2541(93)90042-H)
- European Commission: COM (2020) Critical raw materials resilience: charting a path towards greater security and sustainability. 24. <https://eur-lex.europa.eu/legal-content/EN/TXT/HTML/?uri=CELEX:52020DC0474&from=EN>, last access: 14 October 2020.
- Fei GC, Li BH, Yang JY, Chen X, Luo W, Li YG, Tang WC, Gu CH, Zhong W, Yang GB (2017) Geology, fluid inclusion characteristics and H-O-C isotopes of large Lijiaogou pegmatite spodumene deposit in Songpan-Garze Fold Belt, Eastern Tibet: implications for ore genesis. *Resour Geol* 68(1):37–50. <https://doi.org/10.1111/rge.12145>
- Fei GC, Menute JF, Li YQ, Yang JY, Deng Y, Chen CS, Yang YF, Yang Z, Qin LY, Zheng L, Tang WC (2020a) Petrogenesis of the Lijiaogou spodumene pegmatites in Songpan-Garze Fold Belt, West Sichuan, China: evidence from geochemistry, zircon, cassiterite and coltan U-Pb geochronology and Hf isotopic

- compositions. *Lithos* 364–365:105555. <https://doi.org/10.1016/j.lithos.2020.105555>
- Fei GC, Yang Z, Yang JY, Luo W, Deng Y, Lai YT, Tao XX, Zheng L, Tang WC, Li J (2020b) New precise timing constraint for the Dangba granitic pegmatite type rare- metal deposit, Markam, Sichuan Province, evidence from cassiterite LA-MC-ICP-MS U-Pb dating. *Acta Geol Sin* 94(3):836–849. <https://doi.org/10.1016/j.oregeorev.2021.104441>
- Fei GC, Menuge JF, Chen CS, Yang YL, Deng Y, Li YG, Zheng L (2021) Evolution of pegmatite ore-forming fluid: the Lijiagou spodumene pegmatites in the Songpan-Garze Fold Belt, southwestern Sichuan province, China. *Ore Geol Rev* 139:104441. <https://doi.org/10.1016/j.oregeorev.2021.104441>
- Fu XF, Hou LW, Wang DH, Yuan LP, Liang B, Hao XF, Pan M (2014) Achievements in the investigation and evaluation of spodumene resources at Jiajika in Sichuan, China. *Geol Surv China* 1(3):37–43 (in Chinese with English abstract)
- Fu XF, Yuan LP, Wang DH, Hou LW, Pan M, Hao XF, Liang B, Tang Y (2015) Mineralization characteristics and prospecting model of newly discovered X03 rare metal vein in Jiajika orefield Sichuan. *Min Depos* 34(6):1172–1186 (in Chinese with English abstract)
- Fu XF, Liang B, Zou FG, Hao XF, Hou LW (2021) Discussion on metallogenetic geological characteristics and genesis of rare polymetallic ore fields in western Sichuan. *Acta Geol Sin* 95(10):3054–3068 (in Chinese with English abstract)
- Goodenough KM (2017) Verplanck and Hitzman: rare earth and critical elements in ore deposits. *Miner Depos* 52(1):129–130. <https://doi.org/10.1007/s00126-016-0679-3>
- Hao XF, Fu XF, Liang B (2015) Formation ages of granite and X03 pegmatite vein in Jiajika, western Sichuan and their geological significance. *Min Depos* 34(6):1199–1208 (in Chinese with English abstract)
- Hou ZQ, Tian SH, Xie YL, Yang ZS, Yuan ZX, Yin SP, Yi LS, Fei HC, Zou TR, Bai G, Li XY (2009) The Himalayan Mianning-Dechang REE belt associated with carbonatite-alkalic complex in the eastern Indo-Asian collision zone, SW China. *Ore Geol Rev* 36(1):65–89. <https://doi.org/10.1016/j.oregeorev.2009.03.001>
- Hou JL, Niu SY, Sun AQ (2017) Preliminary study on the origin of spodumene-bearing pegmatite sediments in Jiajika orefield and some enlightenment. *Northwest Geol* 50(1):90–100 (in Chinese with English abstract)
- Hu X, Li H (2021) Research progress and prospect of granitic pegmatite-type lithium deposits. *Chin J Nonferrous Metals* 31(11):3468–3488 (in Chinese with English abstract)
- Hu RZ, Bi XW, Shao SX, Turner G, Burnard PG (1997) He-Ar isotopic systematics of fluid inclusions in pyrite from Machangqing copper deposit, Yunnan. *Chin Sci Bull* 6:503–508 (in Chinese)
- Hu RZ, Burnard PG, Turner G, Bi XW (1998) Helium and Argon isotope systematics in fluid inclusions of Machangqing copper deposit in west Yunnan province, China. *Chem Geol* 146(1):55–63. [https://doi.org/10.1016/S0009-2541\(98\)00003-5](https://doi.org/10.1016/S0009-2541(98)00003-5)
- Hu RZ, Bi XW, Turner G (1999) He-Ar isotopic geochemistry of gold metallogenetic fluid in Ailaoshan gold metallogenetic belts. *Sci Sin* 4:321–330 (in Chinese)
- Hu RZ, Burnard PG, Bi XW, Zhou MF, Pen JT, Su WC, Wu KX (2004) Helium and argon isotope geochemistry of alkaline intrusion-associated gold and copper deposits along the Red River-Jinshajiang fault belt, SW China. *Chem Geol* 203(3):305–317. <https://doi.org/10.1016/j.chemgeo.2003.10.006>
- Hu RZ, Burnard PG, Bi XW, Zhou MF, Peng JT, Su WC, Zhao JH (2009) Mantle-derived gaseous components in ore-forming fluids of the Xiangshan uranium deposit, Jiangxi province, China: evidence from He Ar and C isotopes. *Chem Geol* 266(1):86–95. <https://doi.org/10.1016/j.chemgeo.2008.07.017>
- Hu RZ, Bi XW, Jiang GH, Chen HW, Peng JT, Qi YQ, Wu LY, Wei WF (2012) Mantle-derived noble gases in ore-forming fluids of the granite-related Yaogangxian tungsten deposit, Southeastern China. *Miner Depos* 47(6):623–632. <https://doi.org/10.1007/s00126-011-0396-x>
- Huang T, Fu XF, Ge LQ, Zou FG, Hao XF, Yang R, Xiao RQ, Fan JB (2020) The genesis of giant lithium pegmatite veins in Jiajika, Sichuan, China: insights from geophysical, geochemical as well as structural geology approach. *Ore Geol Rev* 124:103557. <https://doi.org/10.1016/j.oregeorev.2020.103557>
- Jean-Baptiste P, Bougault H, Vangriesheim A, Charlot JL, Radford-Knoery J, Fouquet Y, Needham D, German C (1998) Mantle  $^3\text{He}$  in hydrothermal vents and plume of the Lucky Strike site (MAR 37°17'N) and associated geothermal heat flux. *Earth Planet Sci Lett* 157(1):69–77. [https://doi.org/10.1016/S0012-821X\(98\)00022-3](https://doi.org/10.1016/S0012-821X(98)00022-3)
- Kendrick MA, Burgess R, Patrick RAD, Turner G (2001) Fluid inclusion noble gas and halogen evidence on the origin of Cu-Porphyry mineralising fluids. *Geochim Cosmochim Acta* 65(16):2651–2668. [https://doi.org/10.1016/S0016-7037\(01\)00618-4](https://doi.org/10.1016/S0016-7037(01)00618-4)
- Kesler SE, Gruber PW, Medina PA, Keoleian GA, Everson MP, Wallington TJ (2012) Global lithium resources: relative importance of pegmatite, brine and other deposits. *Ore Geol Rev* 48:55–69. <https://doi.org/10.1016/j.oregeorev.2012.05.006>
- Knoll T, Schuster R, Huet B (2018) Spodumene pegmatites and related leucogranites from the Austroalpine Unit (Eastern Alps, Central Europe): field relations, petrography, geochemistry and geochronology. *Can Mineral* 56(4):489–528. <https://doi.org/10.3749/canmin.1700092>
- Laznicka P (2006) Giant metallic deposits. Springer Berlin Heidelberg, pp 1–732. <https://doi.org/10.1016/j.oregeorev.2014.03.002>
- Li JK, Chou IM (2016) An occurrence of metastable cristobalite in spodumene-hosted crystal-rich inclusions from Jiajika pegmatite deposit, China. *J Geochem Explor* 171:29–36. <https://doi.org/10.1016/j.gexplo.2015.10.012>
- Li JK, Chou IM (2017) Homogenization experiments of crystal rich inclusions in spodumene from Jiajika lithium deposit, China, under elevated external pressures in a hydrothermal diamond-anvil cell. *Geofluids* 2017:1–12. <https://doi.org/10.1155/2017/9252913>
- Li XF, Mao JW, Wang YT, Wang DH (2003) Evidence of noble gas isotopes and halogen for the origin of ore-forming fluids. *Geol Rev* 49(5):513–521 (in Chinese with English abstract)
- Li JK, Wang DH, Fu XF (2006a)  $^{40}\text{Ar}/^{39}\text{Ar}$  ages of the Ke'eryin pegmatite type rare metal deposit, western Sichuan, and its tectonic significances. *Acta Geol Sin* 80(6):843–848 (in Chinese with English abstract)
- Li JK, Wang DH, Fu XF (2006b) Metallogenetic epoch and tectonic implications of Danba pegmatite type muscovite deposit in Sichuan Province, China. *Min Depos* 25(1):95–100 (in Chinese with English abstract)
- Li JK, Wang DH, Zhang DH, Fu XF (2006c) The discovery of silicate daughter mineral-bearing inclusions in the Jiajika pegmatite deposit, western Sichuan, and its significance. *Mineral Depos* 25(S1):131–134 (in Chinese with English abstract)
- Li JK, Wang DH, Zhang DH, Fu XF (2006d) The source of ore-forming fluid in Jiajika pegmatite type lithium polymetallic deposit, Sichuan Province. *Acta Petrol Mineral* 25(1):45–52 (in Chinese with English abstract)
- Li ZL, Hu RZ, Yang JS, Peng JT, Li XM, Bi XW (2007) He, Pb and S isotopic constraints on the relationship between the A-type Qitianling granite and the Furong tin deposit, Hunan Province,

- China. *Lithos* 97(1):161–173. <https://doi.org/10.1016/j.lithos.2006.12.009>
- Li JK, Wang DH, Liu SB, Ying LJ, Wang CH, Chen DL (2008a) SRXRF microprobe study of fluid inclusions for pegmatite deposits in western Sichuan Province. *Geotecton Metallog* 32(3):332–337 (in Chinese with English abstract)
- Li JK, Zhang DH, Wang DH, Zhang WH (2008b) Liquid immiscibility of fluorine-rich granite magma and its diagenesis and metallogenesis. *Geolog Rev* 54(2):175–183 (in Chinese with English abstract)
- Li XF, Wang CZ, Hua RM, Wei XL (2010) Fluid origin and structural enhancement during mineralization of the Jinshan orogenic gold deposit, South China. *Mineral Depos* 45(6):583–597. <https://doi.org/10.1007/s00126-010-0293-8>
- Li GL, Hua RM, Zhang WL, Hu DQ, Wei XL, Huang XE, Xie L, Yao JM, Wang XD (2011) He-Ar isotope composition of pyrite and Wolframite in the Tieshanlong Tungsten Deposit, Jiangxi, China: implications for fluid evolution. *Resour Geol* 61(4):356–366. <https://doi.org/10.1111/j.1751-3928.2011.00172.x>
- Li JK, Liu XF, Wang DH (2014) The metallogenetic regularity of lithium deposit in China. *Acta Geol Sin* 88(12):2269–2283 (in Chinese with English abstract)
- Li JK, Zou TR, Liu XF, Wang DH, Ding X (2015a) The metallogenetic regularities of Lithium deposit in China. *Acta Geol Sin* 89(2):652–670. <https://doi.org/10.1111/1755-6724.12453>
- Li SH, Li JK, Zhang DH (2015b) Application of hydrothermal diamond-anvil cell in fluid inclusions: an example from the Jiajika pegmatite deposit in western Sichuan, China. *Acta Geol Sin* 89(4):747–754 (in Chinese with English abstract)
- Li H, Wu QH, Evans NJ, Zhou ZK, Kong H, Xi XS, Lin ZW (2018) Geochemistry and geochronology of the Banxi Sb deposit: implications for fluid origin and the evolution of Sb mineralization in central-western Hunan, South China. *Gondwana Res* 55:112–134. <https://doi.org/10.1016/j.gr.2017.11.010>
- Li P, Li J, Chou IM, Wang DH, Xiong X (2019) Mineralization epochs of granitic rare-metal pegmatite deposits in the Songpan-Ganzé orogenic belt and their implications for orogeny. *Minerals* 9(5):280. <https://doi.org/10.3390/min9050280>
- Li XF, Tian SH, Wang DH, Zhang HJ, Zhang YJ, Fu XF, Hao XF, Hou KJ, Zhao Y, Qin Y, Yu Y, Wang H (2020) Genetic relationship between pegmatite and granite in Jiajika lithium deposit in western Sichuan: evidence from zircon U-Pb dating, Hf-O Isotope and Geochemistry. *Min Depos* 39(2):273–304 (in Chinese with English abstract)
- Li JK, Wang DH, Zhang DH, Fu XF eds. (2007) Mineralization mechanism and continental geodynamics background of pegmatite type deposits in western Sichuan, China. Atomic Energy Press, Beijing. pp 1–187 (in Chinese with English abstract)
- Li JK (2006) Mineralizing mechanism and continental geodynamics of typical pegmatite deposits in western Sichuan, China. China University of Geosciences, Beijing. pp 22–32 (in Chinese with English abstract)
- Liang B, Fu XF, Tang Y, Pan M, Yuan LP, Hao XF (2016) Granite geochemical characteristics in Jiajika rare metal deposit, western Sichuan. *J Guilin Univ Technol* 36(1):42–49 (in Chinese with English abstract)
- Linnen RL, Lichtervelde MV, Cerny P (2012) Granitic pegmatites as sources of strategic metals. *Elements* 8(4):275–280. <https://doi.org/10.2113/gselements.8.4.275>
- Liu LJ, Fu XF, Wang DH, Hao XF, Yuan LP, Pan M (2015) Geological characteristics and metallogenesis of Jiajika-style rare metal deposits. *Min Depos* 34(6):1187–1198 (in Chinese with English abstract)
- Liu LJ, Wang DH, Yang YQ, Fu XF, Hao XF, Pan M, Tang Q, Chen ZY (2016) Metallogenetic characteristics of X03 rare metal vein in Jiajika of Sichuan. *J Guilin Univ Technol* 36(1):50–59 (in Chinese with English abstract)
- Liu LJ, Wang DH, Dai HZ, Hou JL (2017a) Geochemical characteristics of REE and its implications to X03 superlarge lithium pegmatite vein, Jiajika Sichuan. *Earth Sci* 42(10):1673–1683 (in Chinese with English abstract)
- Liu LJ, Wang DH, Hou KJ, Tian SH, Zhao Y, Fu XF, Yuan LP, Hao XF (2017b) Application of lithium isotope to Jiajika new No 3 pegmatite lithium polymetallic vein in Sichuan. *Earth Sci* 24(5):167–171 (in Chinese with English abstract)
- Liu LJ, Wang DH, Liu XF, Li JK, Dai HZ, Yan WD (2017c) The main types, distribution features and present situation of exploration and development for domestic and foreign lithium mine. *Geol China* 44(2):263–278 (in Chinese with English abstract)
- Liu J, Li WC, Zhu XP, Li C, Zhou Q, Yang FC (2020a) Origin and evolution of ore-forming fluids of the Larong W-(Mo) deposit, eastern Tibet: constraints from fluid inclusions, H-O isotopes, and scheelite geochemistry. *Ore Geol Rev* 124:103620. <https://doi.org/10.1016/j.oregeorev.2020.103620>
- Liu T, Tian SH, Wang DH, Zhang YJ, Li XF, Jieken KLMH, Zhang ZL, Wang YQ, Zhao Y, Qin Y (2020b) Genetic relationship between granite and pegmatite in Kalu'an hard-rock-type lithium deposit in Xinjiang: evidence from zircon U-Pb dating, Hf-O isotopes and whole-rock geochemistry. *Acta Geol Sin* 94(11):3293–3334 (in Chinese with English abstract)
- Liu T, Tian SH, Wang DH, Hou KJ, Zhang YJ, Li XF, Jieken KLMH, Zhang ZL, Wang YQ, Zhao Y, Qin Y (2021) Characteristics of ore-forming fluids in Kalu'an hard-rock-type lithium deposit in Xinjiang Province, China: evidence from He–Ar isotopes. *Geol Rev* 67(6):1697–1708 (in Chinese with English abstract)
- London D (2008) Pegmatites. Min Assoc Canada. <https://doi.org/10.2113/gsecongeo.103.8.1730>
- London D (2014) A petrologic assessment of internal zonation in granitic pegmatites. *Lithos* 184–187:74–104. <https://doi.org/10.1016/j.lithos.2013.10.025>
- Luo W, Peng J, Jin TF, Yang B, Pang LW, Zhou ZM (2022) Genesis and geological significance of Simanco biotite monzogranite in the Ke'eryin area, Western Sichuan, China. *Bull Miner Petrol Geochim* 41(03):527–539 (in Chinese with English abstract)
- Lupton J, Baker E, Massoth G (1989) Variable  $^3\text{He}/\text{heat}$  ratios in submarine hydrothermal systems: Evidence from two plumes over the Juan de Fuca ridge. *Nature* 337(6203):16–164. <https://doi.org/10.1038/337161a0>
- Lupton JE, Baker ET, Massoth GJ, Thomson RE, Burd BJ, Butterfield DA, Embley RW, Cannon GA (1995) Variations in water-column  $^3\text{He}/\text{heat}$  ratios associated with the 1993 CoAxial event, Juan de Fuca Ridge. *Geophys Res Lett* 22(2):155–158. <https://doi.org/10.1029/94GL02797>
- Lv ZH, Zhang H, Tang Y, Guan SJ (2012) Petrogenesis and magmatic-hydrothermal evolution time limitation of Kelumute no.112 pegmatite in Altay, Northwestern China: evidence from zircon U-Pb and Hf isotopes. *Lithos* 154:374–391. <https://doi.org/10.1016/j.lithos.2012.08.005>
- Mamyrin BA, Tolstikhin IN (1984) Helium Isotopes in Nature. Elsevier Science Publishing Company Inc, pp 1–273
- Marty B, Jambon A, Sano Y (1989) Helium isotopes and  $\text{CO}_2$  in volcanic gases of Japan. *Chem Geol* 76(1–2):25–40. [https://doi.org/10.1016/0009-2541\(89\)90125-3](https://doi.org/10.1016/0009-2541(89)90125-3)
- Muller A, Romer RL, Pedersen RB (2017) The Sveconorwegian pegmatite province: thousands of pegmatites without parental granites. *Can Mineral* 55(2):283–315. <https://doi.org/10.3749/canmin.1600075>

- O’Neil JR (1969) Oxygen isotope fractionation in divalent metal carbonates. *J Chem Phys* 51(12):5547–5558. <https://doi.org/10.1063/1.1671982>
- Ozima M, Podosek F (2002) Noble gas geochemistry. Cambridge University Press, Cambridge
- Reid MR, Graham DW (1996) Resolving lithospheric and sub-lithospheric contributions to helium isotope variations in basalts from the southwestern US. *Earth Planet Sci Lett* 144(1):213–222. [https://doi.org/10.1016/0012-821X\(96\)00166-5](https://doi.org/10.1016/0012-821X(96)00166-5)
- Roda-Robles E, Villaseca C, Pesquera A, Gil-Crespo P, Vieira R, Lima A, Garate-Olave I (2018) Petrogenetic relationships between Variscan granitoids and Li-(F-P)-rich aplite-pegmatites in the Central Iberian Zone: geological and geochemical constraints and implications for other regions from the European Variscides. *Ore Geol Rev* 95:408–430. <https://doi.org/10.1016/j.oregeorev.2018.02.027>
- Roger F, Malavieille J, Leloup PH, Calassou S, Xu Z (2004) Timing of granite emplacement and cooling in the Songpan-Garze Fold Belt (eastern Tibetan Plateau) with tectonic implications. *J Asian Earth Sci* 22(5):465–481. [https://doi.org/10.1016/S1367-9120\(03\)00089-0](https://doi.org/10.1016/S1367-9120(03)00089-0)
- Roger F, Jolivet M, Malavieille J (2010) The tectonic evolution of the Songpan-Garze (North Tibet) and adjacent areas from Proterozoic to present: a synthesis. *J Asian Earth Sci* 39:254–269. <https://doi.org/10.1016/j.jseas.2010.03.008>
- Schlutter D, Simmons S, Sawkins F (1987) Mantle-derived helium in two Peruvian hydrothermal ore deposits. *Nature* 329(6138):429–432. <https://doi.org/10.1038/329429a0>
- Shmulovich KI, Landwehr D, Simon K, Heinrich W (1999) Stable isotope fractionation between liquid and vapour in water-salt systems up to 600°C. *Chem Geol* 157(3–4):343–354. [https://doi.org/10.1016/S0009-2541\(98\)00202-2](https://doi.org/10.1016/S0009-2541(98)00202-2)
- Stuart FM, Turner G, Duckworth RC, Fallick A (1994) Helium isotopes as tracers of trapped hydrothermal fluids in ocean-floor sulfides. *Geology* 22(9):823–826. [https://doi.org/10.1130/0091-7613\(1994\)022%3c0823:HIATOT%3e2.3.CO;2](https://doi.org/10.1130/0091-7613(1994)022%3c0823:HIATOT%3e2.3.CO;2)
- Stuart FM, Burnard PG, Taylor RP, Turner G (1995) Resolving mantle and crustal contributions to ancient hydrothermal fluids: He/Ar isotopes in fluid inclusions from Dae Hwa W/Mo mineralization, South Korea. *Geochim Cosmochim Acta* 59(22):4663–4673. [https://doi.org/10.1016/0016-7037\(95\)00300-2](https://doi.org/10.1016/0016-7037(95)00300-2)
- Su AN, Tian SH, Hou ZQ, Li JK, Li ZZ, Hou KJ, Li YH, Hu WJ, Yang ZS (2011) Lithium isotope and its application to Jiajika pegmatite type lithium pokymetallic deposit in Sichuan. *Geoscience* 25(2):236–242 (in Chinese with English abstract)
- Sun XM, Zhang Y, Xiong DX, Sun WD, Shi GY, Zhai W, Wang SW (2009) Crust and mantle contributions to gold-forming process at the Daping deposit, Ailaoshan gold belt, Yunnan China. *Ore Geol Rev* 36(1):235–249. <https://doi.org/10.1016/j.oregeorev.2009.05.002>
- Sun Y, Liu JM, Zeng QD, Wang JB, Wang YW, Hu RZ, Zhou LL, Wu GB, Gao YY, Shen WJ (2017) Geology and hydrothermal evolution of the Baituyingzi porphyry Mo (Cu) deposit, eastern Inner Mongolia, NE China: implications for Mo and Cu precipitation mechanisms in CO<sub>2</sub>-rich fluids. *Ore Geol Rev* 81:689–705. <https://doi.org/10.1016/j.oregeorev.2016.03.023>
- Taylor HP (1974) The application of oxygen and hydrogen isotope studies to problems of hydrothermal alteration and ore deposition. *Econ Geol* 69(6):843–883. <https://doi.org/10.2113/gsecongeo.69.6.843>
- Thomas R, Davidson P, Beurlen H (2012) The competing models for the origin and internal evolution of granitic pegmatites in the light of melt and fluid inclusion research. *Mineral Petrol* 106(1–2):55–73. <https://doi.org/10.1007/s00710-012-0212-z>
- Turner G, Stuart FM (1992) Helium/heat ratios and deposition temperatures of sulphides from the ocean floor. *Nature* 357(6379):581–583. <https://doi.org/10.1038/357581a0>
- Turner G, Burnard PB, Ford JL, Gilmour JD, Lyon IC, Stuart FM, Gruszczynski M, Halliday A (1993a) Tracing fluid sources and interaction: discussion. *Philos Trans Phys Sci Eng* 344(1670):127–140. <https://doi.org/10.1098/rsta.1993.0081>
- Turner S, Hawkesworth C, Liu JQ, Rogers N, Kelley S, Van Calsteren P (1993b) Timing of Tibetan uplift constrained by analysis of volcanic rocks. *Nature* 364(6432):50–54. <https://doi.org/10.1038/364050a0>
- U.S. Geological Survey (2021) Mineral commodity summaries 2021. U.S. Geological Survey, 200. <https://www.usgs.gov/centers/national-minerals-information-center/mineral-commodity-summaries>
- Wang DH, Zou TR, Xu ZQ, Yu JJ, Fu XF (2004) Advance in the study of using pegmatite deposits as the tracer of orogenic process. *Adv Earth Sci* 4:614–620 (in Chinese with English abstract)
- Wang DH, Li JK, Fu XF (2005) <sup>40</sup>Ar/<sup>39</sup>Ar dating for the Jiajika pegmatite-type rare metal deposit in west Sichuan and its significance. *Geochimica* 6:3–9 (in Chinese with English abstract)
- Wang DH, Wang RJ, Li JK, Zhao Z, Yu Y, Dai JJ, Chen ZH, Li DX, Qu WJ, Den MC, Fu XF, Su Y, Zhen GD (2013) The progress in the strategic research and survey of rare earth, rare metal and rare scattered elements mineral resources. *Geol China* 40(2):361–370 (in Chinese with English abstract)
- Wang L, Tang J, Cheng W, Zhang Z, Lin X, Luo MC, Yang C (2015) Origin of the ore-forming fluids and metals of the Bangpu porphyry Mo-Cu deposit of Tibet, China: constraints from He-Ar, H-O, S and Pb isotopes. *J Asian Earth Sci* 103:276–287. <https://doi.org/10.1016/j.jseas.2014.07.041>
- Wang DH, Liu LJ, Dai HZ, Hou JL, Wu XS (2017a) Discussion on particularity and prospecting direction of large and superlarge spodumene deposits. *Earth Sci* 42(12):2243–2257 (in Chinese with English abstract)
- Wang DH, Wang CH, Sun Y, Li JK, Liu SB, Rao KY (2017b) New progresses and discussion on the survey and research of Li, Be, Ta ore deposits in China. *Geol Surv China* 4(5):1–8 (in Chinese with English abstract)
- Wang H, Wang JB, Zhu XY, Li YS, Zhen SM, Sun HR, Chen XY, Hao Y, Sun ZJ, Jiang BB (2018a) Genesis of the Daliangzi Pb-Zn deposit in the western margin of Yangtze Plate: constraints from fluid inclusions and isotopic evidence. *Geotecton Metallog* 42(4):681–698 (in Chinese with English abstract)
- Wang YH, Zhang FF, Liu JJ, Xue CJ, Zhang ZC (2018b) Genesis of the Wurinitu W-Mo deposit, Inner Mongolia, northeast China: Constraints from geology, fluid inclusions and isotope systematics. *Ore Geol Rev* 94:367–382. <https://doi.org/10.1016/j.oregeorev.2018.01.031>
- Wang DH, Dai HZ, Liu SB, Wang CH, Yu Y, Dai JJ, Liu LJ, Yang YQ, Ma SC (2020) Research and exploration progress on lithium deposits in China. *China Geol* 1(3):137–152. <https://doi.org/10.31035/cg2020018>
- Wang Z, Chen ZY, Li JK, Chen YC (2022) Mineralogical characteristics and their constraints on the magmatic-hydrothermal evolution for the Jiajika No 308 pegmatite Western Sichuan, China. *Acta Geol Sin* 96(06):2039–2061 (in Chinese with English abstract)
- Wang DH, Chen YC, Xu ZG, Li TD, Fu XJ (2002) Metallogenesis series and metallogenetic regularity of Altai Mineralization Province. Atomic Energy Press, Beijing. pp 1–493 (in Chinese)
- Weislogel AL, Graham SA, Chang EZ, Wooden J, Gehrels G (2010) Detrital zircon provenance from three turbidite depocenters of the Middle-Upper Triassic Songpan-Garze complex, Central

- China: record of collisional tectonics, erosional exhumation, and sediment production. *Geol Soc Am Bull* 122(11–12):2041–2062. <https://doi.org/10.1130/B26606.1>
- Wen BJ, Fan HR, Hu FF, Liu X, Yang KF, Sun ZF, Sun ZF (2016) Fluid evolution and ore genesis of the giant Sanshandao gold deposit, Jiaodong gold province, China: Constraints from geology, fluid inclusions and H–O–S–He–Ar isotopic compositions. *J Geochem Explor* 171:96–112. <https://doi.org/10.1016/j.gexplo.2016.01.007>
- Wu LY, Hu RZ, Peng JT, Bi XW, Jiang GH, Chen HW, Wang QY, Liu YY (2011) He and Ar isotopic compositions and genetic implications for the giant Shizhuyuan W–Sn–Bi–Mo deposit, Hunan Province, South China. *Int Geol Rev* 53(5–6):677–690. <https://doi.org/10.1080/00206814.2010.510022>
- Xie GQ, Mao JW, Li W, Liu ZhuQQ, HB, Jia GH, Li YH, Zhang J, (2016) Different proportion of mantle-derived noble gases in the Cu–Fe and Fe skarn deposits: He–Ar isotopic constraint in the Edong district, Eastern China. *Ore Geol Rev* 72:343–354. <https://doi.org/10.1016/j.oregeorev.2015.08.004>
- Xiong X, Li JK, Wang DH, Liu LJ, Dai HZ (2019) A study of solid minerals in melt inclusions and fluid inclusions from the Jiajika pegmatite-type lithium deposit. *Acta Petrol Mineral* 38(02):241–253 (**(in Chinese with English abstract)**)
- Xu LL, Bi XW, Hu RZ, Tang YY, Jiang GH, Qi YQ (2014) Origin of the ore-forming fluids of the Tongchang porphyry Cu–Mo deposit in the Jinshajiang–Red River alkaline igneous belt, SW China: constraints from He, Ar and S isotopes. *J Asian Earth Sci* 79:884–894. <https://doi.org/10.1016/j.jseaes.2013.02.013>
- Xu ZQ, Fu XF, Wang RC, Li GG, Zheng YL, Zhao ZB, Lian DY (2020) Generation of lithium-bearing pegmatite deposits within the Songpan–Garze orogenic belt, East Tibet. *Lithos* 354–355:1–11. <https://doi.org/10.1016/j.lithos.2019.105281>
- Xu ZQ, Hou LW, Wang ZX (1992) Orogenic process of Songpan–Garze Orogenic Belt of China. Geological Publishing House, Beijing. 190 (**(in Chinese)**)
- Yan QG, Li JK, Li XJ, Liu YC, Li P, Xiong X (2020) Source of the Zhawulong granitic pegmatite-type lithium deposit in the Songpan–Ganzê orogenic belt, Western Sichuan: constraints from Sr–Nd–Hf isotopes and geochemistry. *Lithos* 378–379:105828. <https://doi.org/10.1016/j.lithos.2020.105828>
- Yang CD, Geng XX, Yang FQ, Li Q (2016) Metallogeny of the Sarsuk polymetallic Au deposit in the Ashele Basin, Altay Orogenic Belt, Xinjiang, NW China: constraints from mineralogy, fluid inclusions, and He–Ar isotopes. *Ore Geol Rev* 100:77–98. <https://doi.org/10.1016/j.oregeorev.2016.10.026>
- Zhai DG, Liu JJ, Ripley EM, Wang JP (2015) Geochronological and He–Ar–S isotopic constraints on the origin of the Sandawanzi gold–telluride deposit, northeastern China. *Lithos* 213:338–352. <https://doi.org/10.1016/j.lithos.2014.11.017>
- Zhai MG, Wu FY, Hu RZ, Jiang SY, Li WC, Wang RC, Wang DH, Qi T, Qin KZ, Wen HJ (2019) Critical metal mineral resources: current research status and scientific issues. *Bull Natl Natural Sci Found China* 33(2):106–111 (**(in Chinese with English abstract)**)
- Zhai YS, Yao SZ, Cai KQ (2011) Mineral deposits. Beijing, Geological Publishing House. 1–413. (**(in Chinese)**)
- Zhang L, Zhang G, Wen H, Qin CJ, Li RX, Zhu CW, Du SJ, Yang G (2018) Genetic implications for the Damajianshan W–Cu–As polymetallic deposit in Lvchun, Southwest China: constraints from H–O, He–Ar, S, and Pb isotopes. *Geol J* 53(S2):384–394. <https://doi.org/10.1002/gj.3187>
- Zhang HJ, Tian SH, Wang DH, Li XF, Liu T, Zhang YJ, Fu XF, Hao XF, Hou KJ, Zhao Y, Qin Y (2021) Lithium isotope behavior during magmatic differentiation and fluid exsolution in the Jiajika granite–pegmatite deposit, Sichuan China. *Ore Geol Rev* 134:104139. <https://doi.org/10.1016/j.oregeorev.2021.104139>
- Zhao ZB, Du JX, Liang FH (2019) Structure and metamorphism of Markam gneiss dome from the eastern Tibetan plateau and its implications for crustal thickening, metamorphism, and exhumation. *Geochem Geophys Geosyst G3* 20(1):24–45. <https://doi.org/10.1029/2018GC007617>
- Zheng YF (1993) Calculation of oxygen isotope fractionation in anhydrous silicate minerals. *Geochim Cosmochim Acta* 57(5):1079–1091. [https://doi.org/10.1016/0016-7037\(93\)90306-H](https://doi.org/10.1016/0016-7037(93)90306-H)
- Zhou X, Zhou Y, Sun BW, Tan HQ, Yue XY, Zhu ZM (2021) Cassiterite U–Pb dating of No 134 pegmatite vein in the Jiajika rare metal deposit, western Sichuan and its geological significances. *Rock Min Anal* 40(01):156–164 (**(in Chinese with English abstract)**)

Springer Nature or its licensor (e.g. a society or other partner) holds exclusive rights to this article under a publishing agreement with the author(s) or other rightsholder(s); author self-archiving of the accepted manuscript version of this article is solely governed by the terms of such publishing agreement and applicable law.